Journal of Green Energy Research and Innovation

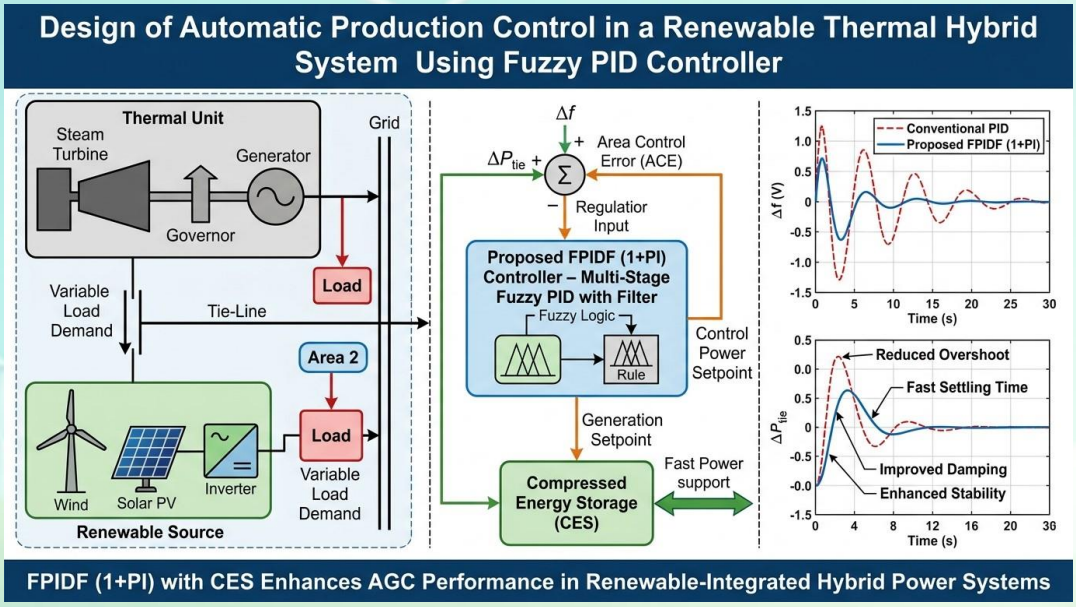
Design of Automatic Production Control in a Renewable Thermal Hybrid System Using Fuzzy PID Controller

Asaad Shemshadi, Mehdi Payamani

Highlights

- **A multi-stage FPIDF (1+PI) controller is proposed for improving AGC stability in renewable hybrid systems.**
- **The AGC model incorporates CES units and excitation system dynamics for more accurate control performance.**
- **The controller reduces overshoot, steady-state error, and enhances robustness under severe load disturbances.**
- **Faster settling time and improved frequency recovery are achieved across complex two-area dynamic scenarios.**

Graphical Abstract



Use your device to scan and read the article online

Citation

A. Shemshadi and M. Payamani, "Design of Automatic Production Control in a Renewable Thermal Hybrid System Using Fuzzy PID Controller," *Journal of Green Energy Research and Innovation*, vol. 3, no. 3, pp. 47-73, 2026.

https://doi.org/10.61882/jgeri.3.3.47

Journal of Green Energy Research and Innovation 3.3 (2026) 47-73

Online ISSN: 3041-9018

Journal of Green Energy Research and Innovation

Journal Homepage: www.jgeri.araku.ac.ir



Design of Automatic Production Control in a Renewable Thermal Hybrid System Using Fuzzy PID Controller

Asaad Shemshadi *, Mehdi Payamani

Department of Electrical Engineering, Arak University of Technology, Arak, Iran.

A R T I C L E I N F O

Keywords:
Renewable energy,
Power system,
Fuzzy logic,
Automatic Generation Control.

Article History:
Received: 18 August 2025;
Revised: 04 October 2025;
Accepted: 23 October 2025.

Article type:
Research Article

* *Corresponding author*
E-mail address:
shemshadi@arakut.ac.ir (A. Shemshadi)

A B S T R A C T

Power systems integrated with renewable energy sources represent inherently complex and nonlinear structures, often subject to significant frequency deviations and power oscillations, particularly during periods of production shortfall under dynamic and high-load conditions. Furthermore, continuous fluctuations in load demand contribute to variations in grid frequency, transmission line power flow, and the output of generation units. To address these challenges, modern power grids employ Automatic Generation Control (AGC) systems. AGC functions to restore system frequency to its nominal value by utilizing a control metric known as the Area Control Error (ACE), while also ensuring that scheduled inter-area power transfers are maintained at their predefined levels. Achieving production balance in such situations is highly challenging. To address this issue, advanced control techniques and rapid energy storage systems (ESS) are required. ESS units, such as Capacitive Energy Storage (CES) systems, exhibit remarkable capabilities in balancing production demand and grid frequency demand. These systems effectively reduce power frequency oscillations caused by sudden and variable load disturbances, thereby regulating the frequency of the power system. Accordingly, this study investigates the influence of CES units on the performance of AGC within a robust, interconnected power system. Given that fuzzy control methodologies are known to outperform traditional techniques under highly dynamic and uncertain operational environments, a novel multi-stage intelligent fuzzy Proportional-Integral-Derivative controller with an integrated filter (1 + PI), referred to as FPIDF (1 + PI), is proposed. This advanced control strategy aims to improve the overall effectiveness and stability of AGC operations. Simulation outcomes substantiate the enhanced performance of the proposed controller relative to conventional approaches.

1. Introduction

In this chapter, the automatic generation control (AGC) system and its operation will be introduced. Prior to that, to familiarize readers with the performance of various grid components in response to load changes, the load-frequency control (LFC) system will be explained. The topic of AGC has always been one of the most critical discussions in power systems. Given that load variations occur continuously, it is essential for production to be adjusted automatically through a mechanism that regulates power output [1]. If AGC is not implemented in a power system, even with appropriate design, the power grid will still face challenges [2]. Optimal operation of power systems necessitates that frequency changes remain within specific limits, ensuring frequency stability which reflects the balance between production and consumption [3]. AGC was first employed approximately 40 years ago. Initially, the AGC system was analog and very simple [4]. However, with the growth of various loads and power generation sources in modern power grids, the AGC system has evolved from a limited-function analog system to a digital system with extensive capabilities [5]. Designed AGC systems must operate based on unified criteria and control standards. For this purpose, standards have been developed by the North American Electric Reliability Corporation (NERC) [6].

The first studies on AGC are available in Ref. [7-10], and standard definitions of AGC have also been published by IEEE [11]. Additionally, the first design for optimal frequency control in an interconnected network was conducted and documented in Ref. [12,13].

In recent years, various methods have been employed for LFC in power systems. All these methods aim to reduce frequency deviations during dynamic and steady-state conditions [14]. One of the proposed methods for LFC is variable structure control, which improves system response to load variations through various algorithms [15-17]. Another method presented in recent years involves using robust controllers. Combining this type of controller with others aims to design compensators that ensure frequency stability in systems, even with changes in operating points. This approach has been employed in past years [18-20].

More recently, proposals for dynamic modeling and refinement of AGC definitions have been presented, considering physical limitations and network changes [21]. Intelligent control methods, such as neural networks [22] and fuzzy control [23], have also been suggested to address the challenges. Ref. [24-27] propose an intelligent controller based on fuzzy logic and neural networks for generation control in a two-area thermal-hydro system.

In Ref. [28], a Deep Reinforcement Learning (DRL)-based $H\infty$ robust controller is designed to improve frequency stability in a power system that includes Offshore Wind Farms (OWFs). This method seeks to mitigate the negative effects of the OWFs on system inertia and stabilize frequency by incorporating Virtual Inertia Control (VIC) for the wind farms. The performance of this $H\infty$–DRL method is compared with DMPC and PID controllers in various scenarios. However, $H\infty$ controllers may not perform optimally against uncertainties outside the predefined range, and their design is inherently complex. Additionally, implementing Deep Reinforcement Learning requires extensive training data and precise neural network tuning, which can be challenging.

Ref. [29] presents a novel control approach based on a cascaded Fuzzy Optimal Proportional–Derivative controller (FOPD)– Fuzzy Optimal Proportional–Integral–Derivative (FOPID) controller for the coordinated control of LFC and a Superconducting Magnetic Energy Storage (SMES) system in a power system featuring a wind turbine. To enhance performance, the parameters of this controller are optimized using a new metaheuristic algorithm called the Developed Owl Search Algorithm (DOSA). The method's performance is compared with several other controllers, including a robust controller and a PID optimized by the MSA algorithm. This approach demonstrates robust performance against load disturbances, wind turbine disturbances, and system parameter uncertainties, as well as high convergence speed in the optimization algorithm and a significant improvement in frequency stability. However, in cascaded controllers, the computational complexity and the tuning of multiple parameters in both fractional-order controllers and metaheuristic optimization algorithms can be time-consuming and challenging. Ref. [30] addresses the issue of frequency stability in a power system with wind turbines and communication time delays. To overcome the problem of low damping speed of frequency oscillations, a method based on Virtual Damping for wind turbines is proposed. This method actively participates in frequency control by receiving feedback from the frequency deviation, and its performance is compared with conventional methods (without virtual damping). One limitation of this method is that a portion of the wind turbine's generation capacity (5% in this paper) must be reserved as reserve power for implementing virtual damping. Furthermore, the value of the virtual damping gain is determined by trial and error based on system experiments, which may not be optimal under different operating conditions.

The Main Contributions and Innovations of This Research are as follows:

- Designing an FPID with Filter (FPIDF (1 + PI)): Introducing a multi-stage FPIDF controller integrated with a compensator filter (1 + PI) to enhance AGC stability in hybrid power systems.
- Integrating CES and Excitation System Dynamics: Simultaneously incorporating the effects of CES systems and the dynamic characteristics of Excitation Systems within the AGC model to achieve more accurate simulation and a more effective control strategy under realistic conditions.
- Enhancing Stability and Robustness: Demonstrating the proposed method's superiority in reducing overshoot, minimizing steady-state error, and improving robustness against severe load disturbances compared to conventional AGC controllers.
- Evaluating under Complex Scenarios: Investigating the performance of the two-area model, which contains renewable energy sources, under rigorous dynamic scenarios, including sudden load changes in one area, load changes in the other area, and the simultaneous application of load changes in both areas.
- Improving Frequency Performance Metrics: Achieving a shorter settling time and a more stable frequency recovery, which confirms the FPIDF controller's effectiveness in successfully managing frequency deviations in grids with high renewable energy fluctuations.

1.1. AGC in the Iranian Grid

The Iranian national electricity grid, based on data obtained from the Tavanir Operation Office, has an approximate nominal capacity of 70,000 MW. It includes around 120 power plants, 335 transmission substations of 400 kV and 230 kV, and a 48,000 km network of 400 kV and 230 kV lines. Frequency control has always been one of the critical challenges in the Iranian national grid.

In the past, the Dez hydropower plant was used to control frequency across the national grid. The Dez dam power plant consists of eight generating units, each with a capacity of 65 MW. To control the frequency, one of the units at Dez Power Plant was set to a droop-free mode with its generation adjusted to 30 MW. When the load in the grid changed, this unit would handle all the load variations to maintain the nominal frequency of 50 Hz. Subsequently, its generation was manually adjusted by increasing or decreasing the output of other units in the Dez Power Plant, returning its generation to 30 MW. This setup allowed the unit to continue responding to increases or decreases in generation needed to restore the grid frequency to its nominal value.

On May 20, 2001, at 12:00 noon, a fault occurred on the 400 kV Salimi-Ahavan line between Neka Power Plant and Tehran. With the second line between Neka and Jaleh substations out of service, this incident, followed by subsequent events, led to a nine-hour blackout in Iran's electricity network. Similarly, on April 1, 2003, at 9:20 PM, a single-phase fault occurred on the 230 kV line between Anjirek Arak substation (serving as the bridge between the northern and southern grids) and Arak-2 substation. This fault, along with the explosion of a circuit breaker at Anjirek substation and the ensuing events, caused another nationwide blackout in the Iranian power grid.

The two major blackouts highlighted above, alongside the growing importance of identifying and resolving network deficiencies, created conditions that initiated the "Comprehensive Studies of the National Power Grid" project in 2004. This project aimed to reduce the likelihood of such events. Among 11 contractors, Siemens was ultimately chosen to implement this plan.

As part of this initiative, the automatic frequency control system was introduced in the Iranian grid. Using this system, an automatic intra-regional generation control system (i.e., AGC) was deployed to restore frequency to its nominal value. The implemented AGC sent control signals to five power plants in the national grid, including:

- Shahid Mofateh Power Plant, consisting of 4 steam units with a capacity of 250 MW each;
- Shahid Rajaei Steam Power Plant, consisting of 4 units of 250 MW each;
- Bandar Abbas Power Plant, consisting of 4 steam units with a capacity of 320 MW each;
- Toos Power Plant, consisting of 4 steam units with a capacity of 150 MW each;
- Dez Hydropower Plant, consisting of 8 units of 65 MW each.

The implemented AGC sent signals to all units in the mentioned power plants. Its operation commenced three seconds after an event and concluded within 15 minutes. However, at present, this AGC system has been decommissioned, likely due to unsatisfactory performance.

2. LFC System

2.1. Real Power and Frequency Control

After the initial oscillations caused by a disturbance in a power system (e.g., an additional load request), the system stabilizes at a new operating point. To restore the frequency, voltage, and line transfer powers to acceptable ranges, real and reactive power control systems are employed. Although real and reactive powers are not entirely independent of each other, power systems are often designed with two separate control systems for managing these variables. By increasing or decreasing the real power output of various units, either manually or automatically, the network frequency and the real power transmitted through the lines are controlled. On the other hand, by adjusting the reactive power output in different parts of the network, the voltage at different nodes and the reactive power of the lines are regulated [9].

For a power system to perform satisfactorily, the frequency must remain nearly constant. Accurate frequency control ensures the stability of induction and synchronous motor speeds, which is essential for satisfactory operation of generating units. These units rely heavily on auxiliary drives related to fuel, feed water, and air supply systems. In a network, a significant frequency drop can cause severe magnetic currents in induction motors and transformers. Moreover, the widespread use of electric clocks and the utilization of frequency for other timing purposes necessitate maintaining precise synchronization, achieved through accurate frequency control.

2.2. Basic Principles of Speed Control

In a power system, governing devices are installed on generating units to maintain the balance between generated power and load demand, as shown in Figure 1. When a load increases or decreases, the turbine speed changes, leading to a frequency deviation. The governing device adjusts the turbine input to restore the speed to its nominal value.

For synchronous generators, speed variations are directly related to frequency changes. Therefore, controlling speed also ensures frequency regulation. Most turbines are equipped with speed governors that use proportional control systems to adjust the turbine's fuel input based on frequency deviations. However, these proportional governors exhibit steady-state errors, as they do not entirely eliminate frequency deviations caused by load variations.

2.3. Generator Response to Load Changes

When a load increases in the system, the immediate response comes from the kinetic energy stored in the rotating masses of the generator-turbine system. This leads to a decrease in system frequency. The governor responds to this frequency deviation by increasing the turbine's input power to restore the balance between generation and demand.

The response of the generator-turbine system to load changes depends on factors such as the governor's settings, the system's inertia, and the speed of the control system. A fast and accurate response is crucial to maintaining frequency stability and preventing prolonged frequency deviations. This is presented in Figure 2.

In load-frequency studies, the above relationship is expressed in terms of electrical and mechanical powers instead of torque. The relationship between power P and torque T is as Equation (1) [9]:

$$P = \omega_r T \tag{1}$$

Considering a small deviation from the initial values, this relationship can be written as Equation (2):

$$\begin{aligned} P &= P_0 + \Delta P \\ T &= T_0 + \Delta T \\ \omega_r &= \omega_0 + \Delta\omega_r \end{aligned} \tag{2}$$

By putting these relationships into the power and torque relationship, we arrive at Equation (3):

$$P_0 + \Delta P = (\omega_0 + \Delta\omega_r)(T_0 + \Delta T) \tag{3}$$

By simplifying and ignoring higher-order terms, the relationship between the changes in values is as Equation (4):

$$\Delta P = \omega_0 \Delta T + T_0 \Delta\omega_r \tag{4}$$

So, we have Equation (5):

$$\Delta P_m - \Delta P_e = \omega_0(\Delta T_m - \Delta T_e) + (T_{m0} - T_{e0})\Delta\omega_r \tag{5}$$

In steady state, the electrical and mechanical torques are equal. Also, if the speed is expressed in units, then Equation (6) will be obtained:

$$\Delta P_m - \Delta P_e = \Delta T_m - \Delta T_e \tag{6}$$

Speed and power conversion function is shown in Figure 3.

2.4. Load Response to Frequency Deviations

The load on the power system is composed of various components, including resistive, inductive, and motor loads. Frequency deviations affect the performance of these components. For instance, the speed of induction motors decreases with frequency, reducing their power consumption. Conversely, resistive loads are generally unaffected by frequency changes.

The overall response of the load to frequency deviations is quantified using a load-frequency sensitivity coefficient, which indicates how much the load changes with a given frequency deviation. This coefficient is essential in designing effective frequency control strategies for the power system. Block diagram considering load damping and its reduced version are shown in Figures 4 and 5, respectively.

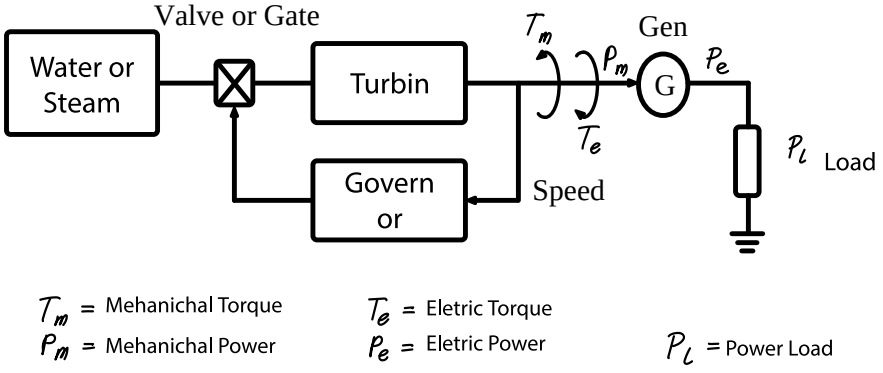


Figure 1. A generator supplying a single load [9].

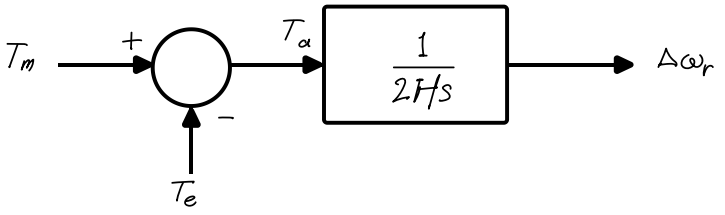


Figure 2. Speed and torque conversion function [9].

2.5. Constant Speed Governor

In power systems, a constant-speed governor is utilized to maintain a steady operating frequency. This type of governor ensures that the turbine operates at a constant speed, regardless of load changes, by adjusting the turbine input accordingly. The performance of a constant-speed governor is evaluated based on its ability to maintain frequency stability under various operating conditions. However, this type of governor may experience steady-state errors when significant load variations occur, as it lacks the ability to entirely eliminate frequency deviations. Constant speed governor diagram is depicted in Figure 6. Generator response diagram with constant speed governor is given in Figure 7, and schematic representation of governor components is provided in Figure 8.

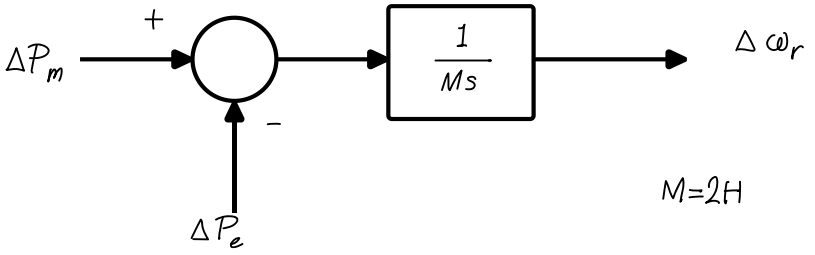


Figure 3. Speed and power conversion function [9].

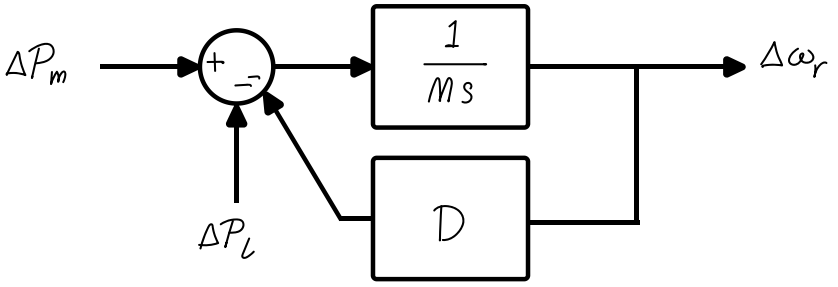


Figure 4. Block diagram considering load damping [10].

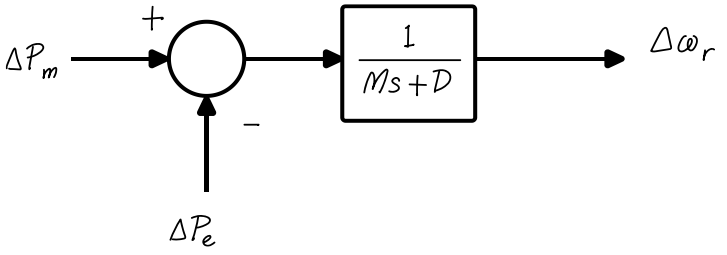


Figure 5. Reduced block diagram considering load damping [10].

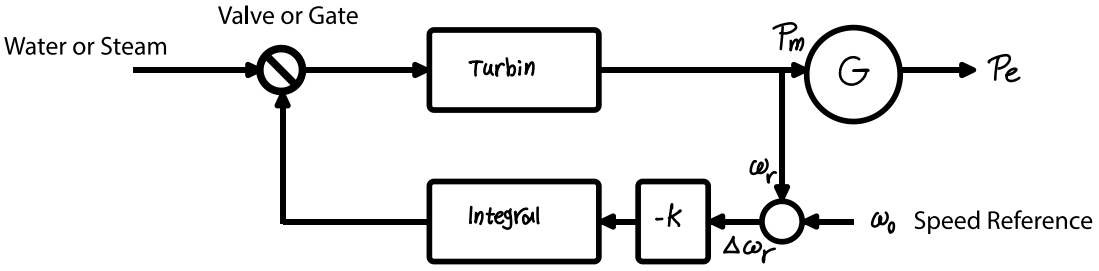


Figure 6. Constant speed governor diagram [11].

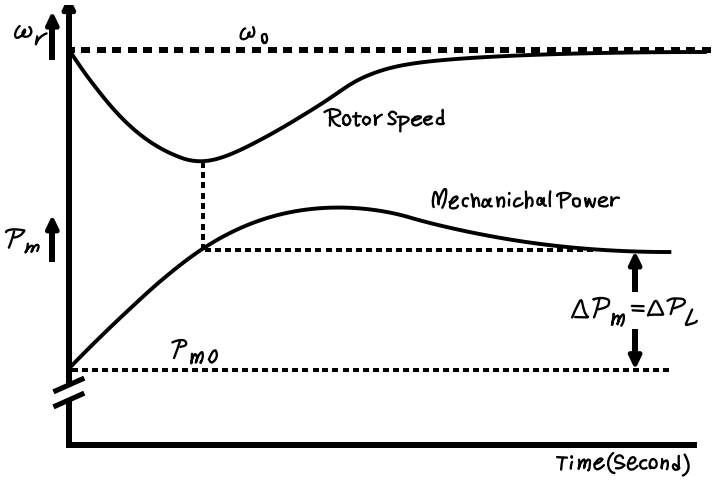


Figure 7. Generator response diagram with constant speed governor [11].

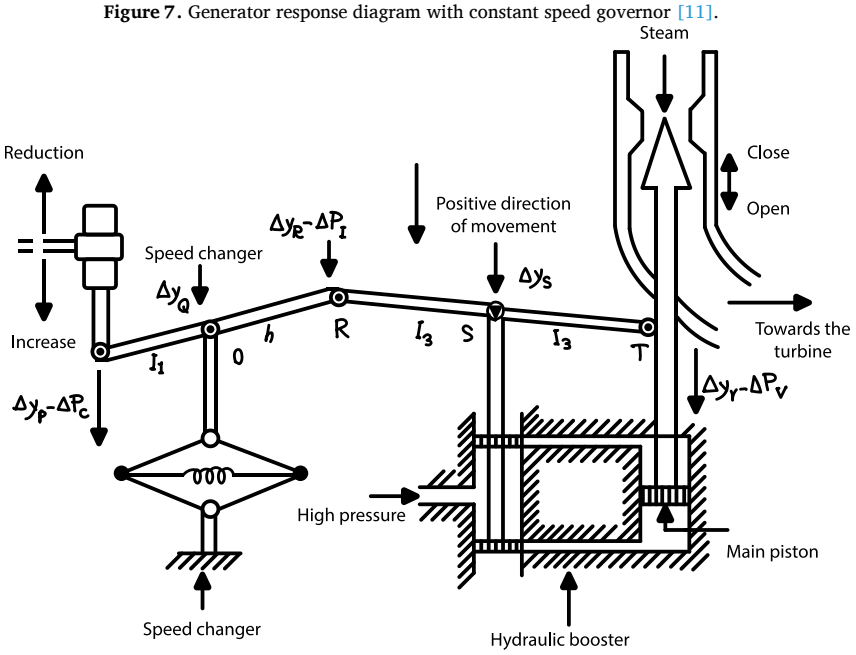


Figure 8. Schematic representation of governor components [11].

2.6. Governor with Droop Characteristics

Governors equipped with droop characteristics allow for proportional changes in turbine speed and frequency as load varies. This feature enables multiple generating units to share the load proportionally based on their respective capacities.

The droop characteristic is defined as the percentage change in speed (or frequency) required to achieve a full load change. For example, a governor with a 5% droop implies that a 5% change in frequency results in a transition from no load to full load. This proportional response is essential for maintaining system stability when multiple generators operate in parallel. Governor with steady-state feedback is given in Figure 9, and Block diagram of a speed governor with a decreasing slope is shown in Figure 10.

2.7. Speed Regulation Percentage or Droop

The speed regulation percentage, also referred to as droop, is a critical parameter in the design of governors. It determines how much the turbine's output changes with frequency deviations. Lower droop values result in a more sensitive governor response, while higher droop values provide better stability but less sensitivity. In systems with multiple generators, the droop setting must be coordinated to ensure an equitable load distribution. This coordination prevents any single generator from becoming overloaded while others remain underutilized. Steady-state characteristic of a governor with a falling slope is given in Figure 11.

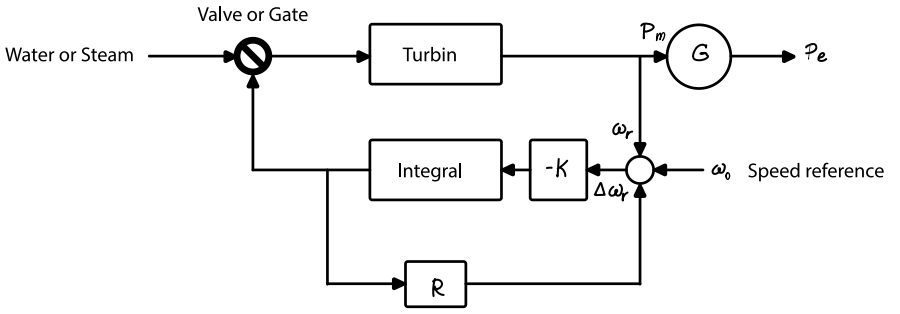
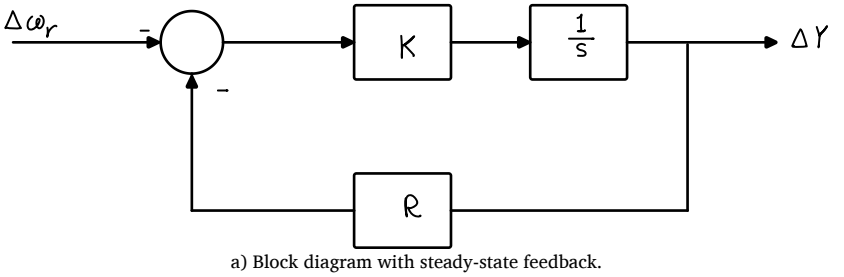
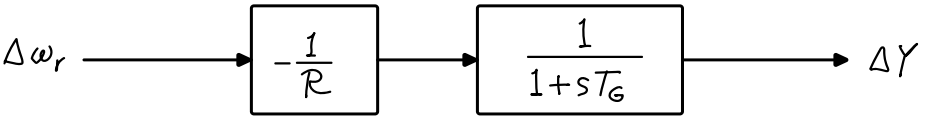


Figure 9. Governor with steady-state feedback [12].



a) Block diagram with steady-state feedback.



b) Reduced block diagram.

Figure 10. Block diagram of a speed governor with a decreasing slope [26].

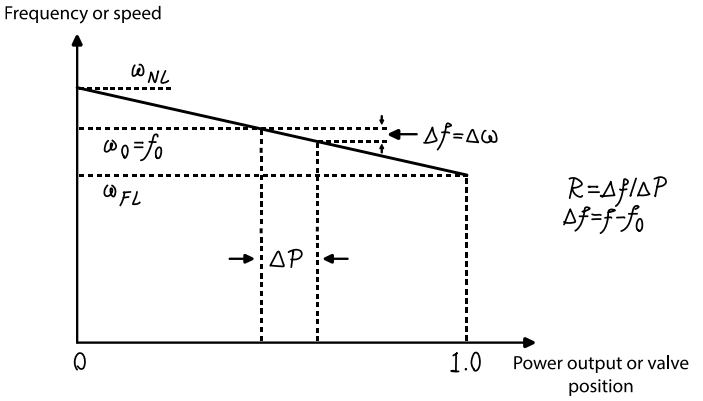


Figure 11. Steady-state characteristic of a governor with a falling slope [6].

2.8. Load Sharing Among Parallel Units

In a power system with parallel generating units, load sharing is achieved through coordinated governor action. The governors of individual units adjust their outputs proportionally to their capacities and droop settings, ensuring an even distribution of the total load.

This proportional load sharing mechanism is essential for maintaining system reliability and preventing overloading of specific units. Additionally, it enhances system resilience by allowing for the seamless addition or removal of generators without disrupting frequency stability. Power division in parallel units with a falling slope governor is given in Figure 12. Governor response diagram with a falling slope is provided in Figure 13.

2.9. Output Power Control of Generating Units

The output power of generating units is controlled to match the load demand while maintaining system frequency. This control involves adjusting the turbine input based on real-time frequency deviations and load changes.

Advanced control systems, such as AGC, further enhance the precision and responsiveness of output power control. These systems use real-time data to optimize generator performance and ensure frequency stability across the entire grid. Governor with load reference set point is given in Figure 14. Effect of the set point on the governor characteristic is presented in Figure 15.

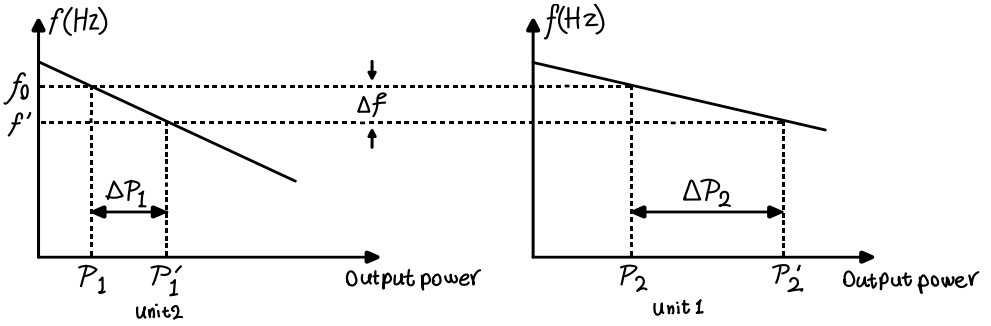


Figure 12. Power division in parallel units with a falling slope governor [11].

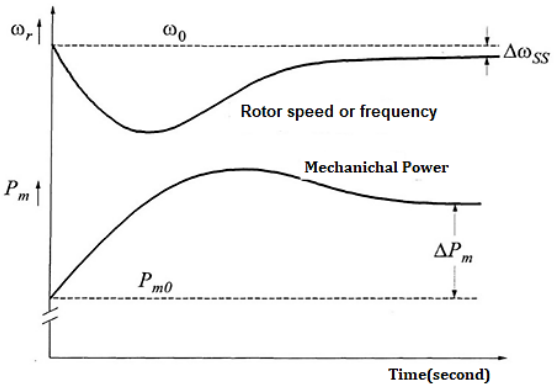


Figure 13. Governor response diagram with a falling slope [11].

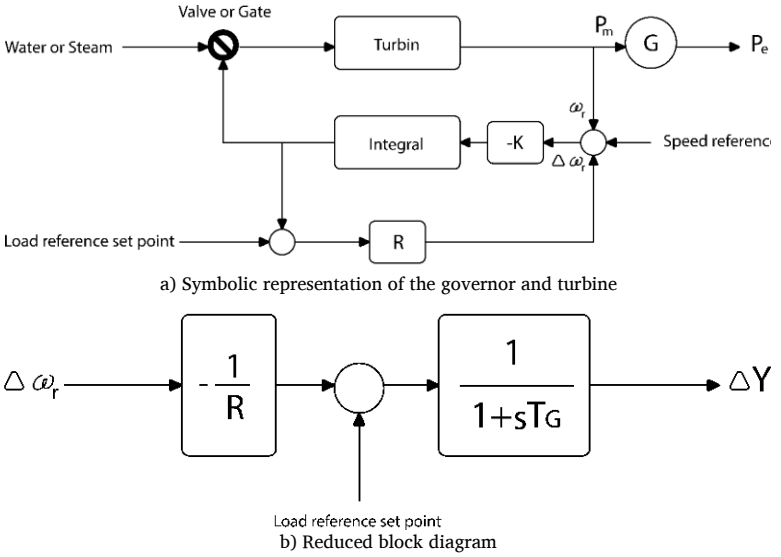


Figure 14. Governor with load reference set point [12].

2.10. Realistic Speed Droop Characteristics

In practical power systems, the speed droop characteristics of governors are influenced by factors such as system inertia, turbine dynamics, and load sensitivity. These factors must be considered when designing governors to ensure accurate frequency regulation.

Realistic droop characteristics account for these dynamic factors, allowing governors to provide stable and reliable frequency control even under fluctuating load conditions.

2.11. Combined Characteristics of Power System Regulation

The combined regulation characteristics of a power system are determined by the collective droop settings and response times of all participating generators. These characteristics play a crucial role in maintaining system stability and ensuring equitable load sharing among generators.

By analyzing these combined characteristics, system operators can identify potential areas for improvement and implement control strategies to enhance overall system performance.

Actual and ideal characteristics of a governor with a decreasing speed slope are provided in Figure 16. Total network equivalent for load-frequency analysis is shown in Figure 17. Governor and load combination characteristic is given in Figure 18. Also, block diagram of a steam turbine generation unit with reheater is presented in Figure 19.

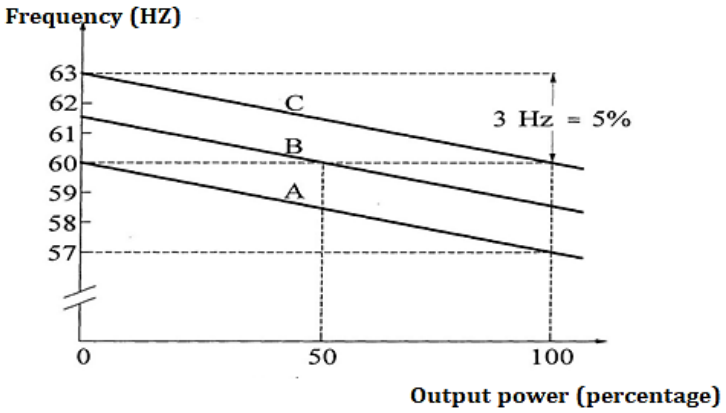


Figure 15. Effect of the set point on the governor characteristic [12].

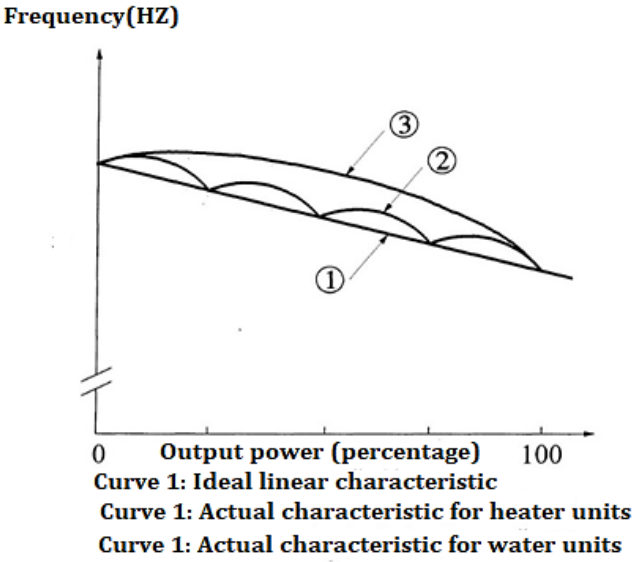


Figure 16. Actual and ideal characteristics of a governor with a decreasing speed slope [23].

For a system with n generators and a combined load damping constant D, the steady-state frequency deviation following a load change is equal to Equation (7) [11]:

$$\Delta f_{ss} = \frac{-\Delta P_L}{\left(\frac{1}{R_1}+\frac{1}{R_2}+\ldots+\frac{1}{R_n}\right)+D} = \frac{-\Delta P_L}{\frac{1}{R_{eq}}+D} \tag{7}$$

And, we have Req as given by Equation (8):

$$R_{eq} = \frac{1}{\frac{1}{R_1}+\frac{1}{R_2}+\ldots+\frac{1}{R_n}} \tag{8}$$

Therefore, the combined frequency response characteristic of the system is as Equation (9):

$$\beta = \frac{-\Delta P_L}{\Delta f_{ss}} = \frac{1}{R_{eq}} + D \tag{9}$$

The system frequency response characteristic (β) is usually expressed in terms of Mw/Hz. This parameter is also sometimes referred to as the system stiffness. The system tuning characteristic is equal to 1/ β.

Figure 18 shows the effect of governor speed reduction and load frequency sensitivity on the net load change, which shows the combined effect of all the generating and load units in the system. An increase in system load by (at rated frequency) leads to an increase in total generation by (due to governor action) and a decrease in total load by (due to its frequency-sensitive characteristic) [10].

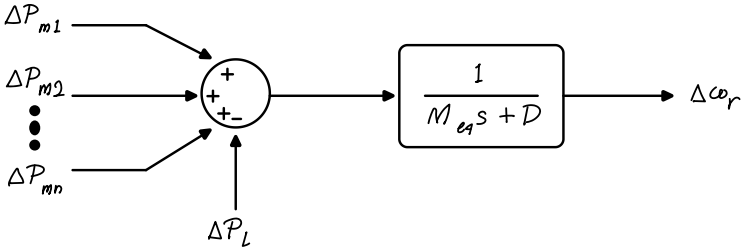


Figure 17. Total network equivalent for load-frequency analysis [12].

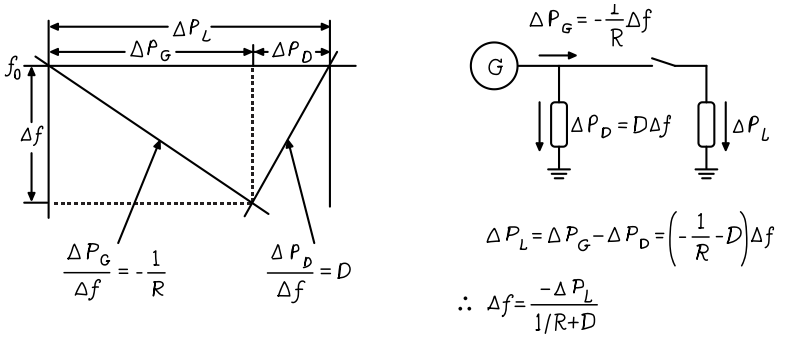
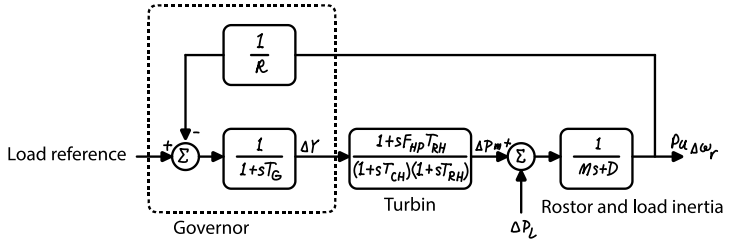


Figure 18. Governor and load combination characteristic [12].



Typical values:

$R = 0.05$	$T_G = 0.2\ s$	$F_{HP} = 0.3$	$T_{RH} = 7.0\ s$
$T_{CH} = 0.3\ s$	$F_{LP} = 0.7$	$M = 10.0\ s$	$D = 1.0$

Figure 19. Block diagram of a steam turbine generation unit with reheater [27].

2.12. Rate of Response in Governor-Turbine Systems

The rate of response in governor-turbine systems is a critical factor influencing the overall stability and performance of a power system. This rate determines how quickly the turbine can adjust its output in response to frequency deviations caused by load changes.

A faster response rate allows for more effective frequency regulation, particularly during sudden load variations. However, overly aggressive response rates can introduce oscillations and instability. Therefore, a balance must be achieved between speed and stability in designing governor-turbine systems. Turbine conversion function without reheater is given in Figure 20. Block diagram of the hydropower generation unit is shown in Figure 21. Response of heating and water units to load increase can be found in Figure 22.

2.13. Introduction to AGC

AGC is a vital component of modern power systems, designed to maintain frequency stability and manage power flows between interconnected areas. By continuously monitoring frequency and inter-area power flows, AGC adjusts the output of generating units to restore system balance.

AGC operates based on the concept of Area Control Error (ACE), which quantifies the discrepancy between actual and desired power flows and frequency. The primary objectives of AGC include:

- Restoring system frequency to its nominal value.
- Maintaining scheduled power exchanges between control areas.
- Ensuring equitable load sharing among generators.

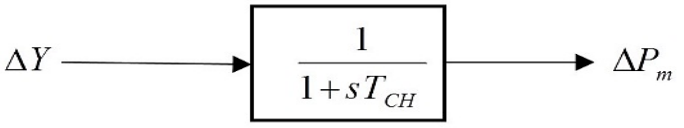
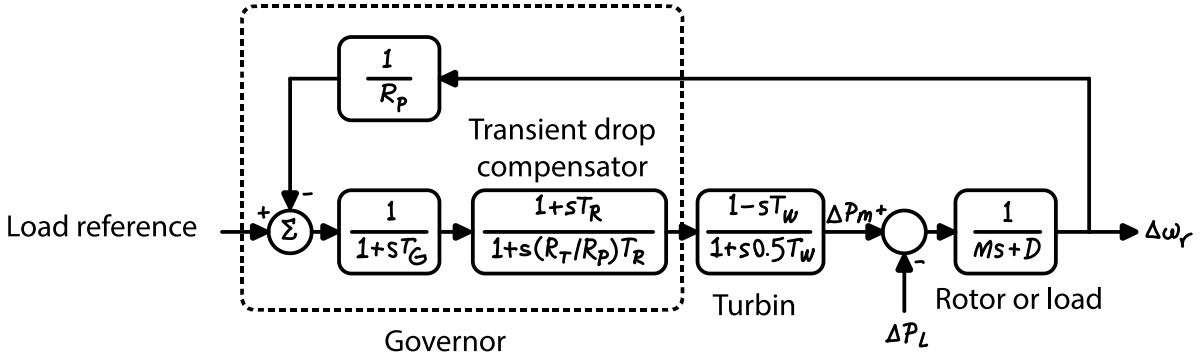


Figure 20. Turbine conversion function without reheater [16].



Typical values:

$R_P = 0.05$ $T_G = 0.2\,s$ $M = 6.0\,s$ $D = 1.0$

$T_W = 1.0_s$ $R_T = 0.38$ $T_R = 5.0_s$

Figure 21. Block diagram of the hydropower generation unit [16].

2.14. AGC in Isolated Grids

In isolated grids, AGC focuses on maintaining frequency stability within a single control area. Without the presence of interconnections to other areas, the responsibility for frequency regulation lies entirely within the isolated grid.

This requires precise coordination among the generating units to ensure that the total generation matches the load demand. AGC in isolated grids often employs advanced algorithms to optimize generator performance and minimize frequency deviations. Additional integral control over the selected generation unit for AGC is shown in Figure 23.

2.15. AGC in Multi-Area Power Systems

In multi-area power systems, AGC plays a crucial role in coordinating power flows between interconnected areas. Each area operates with its own set of generating units and control systems, but they are linked through tie-lines that facilitate power exchange.

The primary objective of AGC in multi-area systems is to maintain scheduled tie-line power flows while ensuring frequency stability in all areas. This is achieved by continuously adjusting the output of generators based on ACE values for each control area. Structure of AGC operation in the network is given in Figure 24.

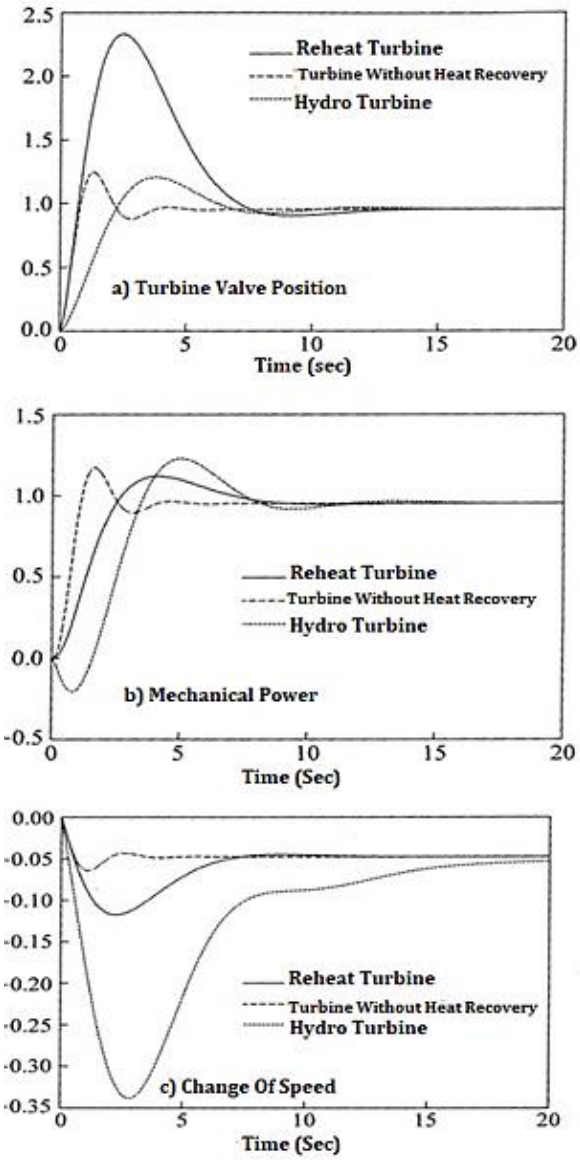


Figure 22. Response of heating and water units to load increase [26].

2.16. AGC in Two-Area Power Systems

In two-area power systems, AGC manages the balance between two interconnected control areas. The tie-line power flows and frequency deviations in each area are monitored and controlled to maintain system stability. The control strategy involves minimizing the ACE in both areas while considering the dynamics of tie-line power flows. This requires precise tuning of the AGC parameters to achieve optimal performance and prevent oscillations. Bi-regional network and its equivalent circuit are shown in Figures 26 and 27.

The steady-state frequency deviation is the same for both regions, and for the total load change it is given as Equation (10) [10]:

$$\Delta f = \frac{-\Delta P_L}{\left(\frac{1}{R_1}+\frac{1}{R_2}\right)+(D_1+D_2)} \tag{10}$$

Consider the steady state values following an increase in the load of zone 1 to be equal. Then for zone 1, Equation (11) holds [10]:

$$\Delta P_{m1} - \Delta P_{12} - \Delta P_{l1} = \Delta f D_1 \tag{11}$$

And for area 2, we have Equation (12):

$$\Delta P_{m2} + \Delta P_{12} = \Delta f D_2 \tag{12}$$

Diagram of a two-zone network with initial speed control is provided in Figure 26.

The change in mechanical power depends on the setting, so we have Equation (13) [10]:

$$\Delta P_{m1} = -\frac{\Delta f}{R_1}$$
$$\Delta P_{m2} = -\frac{\Delta f}{R_2} \tag{13}$$

By substituting the above equations, Equations (14) and (15) are established:

$$\Delta f\left(\frac{1}{R1}+D_1\right) = -\Delta P_{12} - \Delta P_{L1} \tag{14}$$

$$\Delta f\left(\frac{1}{R_2}+D_2\right) = -\Delta P_{12} \tag{15}$$

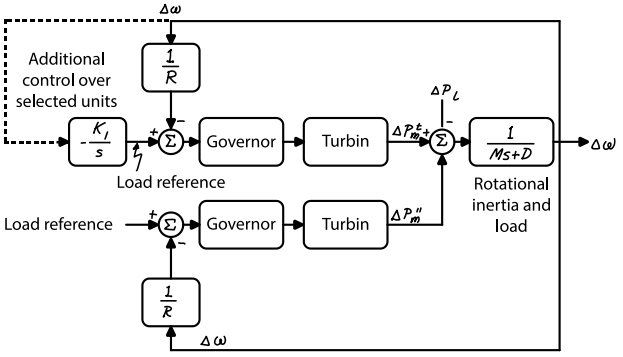


Figure 23. Adding integral control over the selected generation unit for AGC [26].

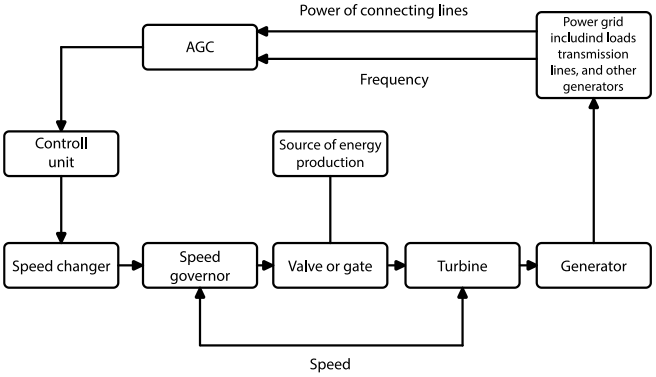


Figure 24. Structure of AGC operation in the network [26].

By solving these equations, we arrive at the following results given by Equation (16):

$$\Delta f = \frac{-\Delta P_{L1}}{\left(\frac{1}{R1}+D_1\right)+\left(\frac{1}{R_2}+D_2\right)} = \frac{-\Delta P_{L1}}{\beta_1+\beta_2}$$
$$\Delta P_{12} = \frac{-\Delta P_{L1}\left(\frac{1}{R_2}+D_2\right)}{\left(\frac{1}{R1}+D_1\right)+\left(\frac{1}{R_2}+D_2\right)} = \frac{-\Delta P_{L1}\,\beta_2}{\beta_1+\beta_2} \quad (16)$$

Where β1 and β2 are the combined frequency response characteristics of regions 1 and 2, respectively. The above relationships are depicted in Figure 27.

Similarly, for the load change in region 2, we have Equation (17) [10]:

$$\Delta f = \frac{-\Delta P_{L2}}{\beta_1+\beta_2}$$
$$\Delta f = \frac{-\Delta P_{L2}}{\beta_1+\beta_2} \quad (17)$$

The above relationships represent the basis of LFC of interconnected systems [7].

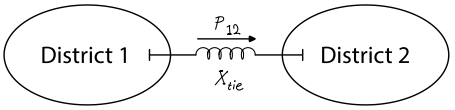


Figure 26. Bi-regional network [4].

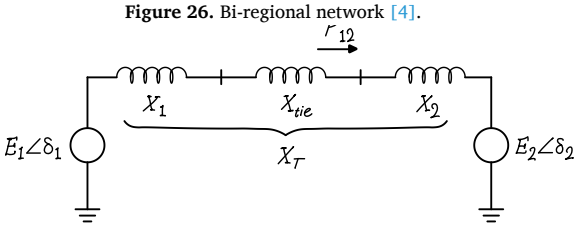


Figure 25. Equivalent circuit of a two-zone network [4].

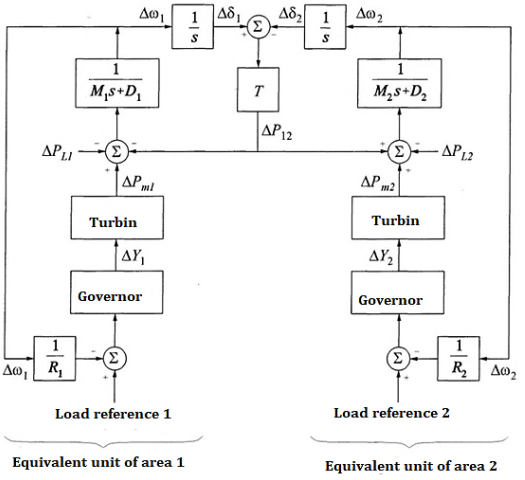


Figure 26. Two-zone network with initial speed control [10].

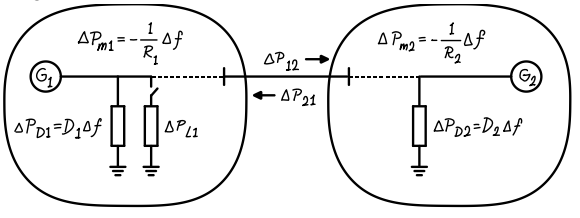


Figure 27. Effect of change in load of zone 1.

2.17. Frequency Bias Control of Tie-Line Power Flows

Frequency bias control is a key aspect of AGC that ensures stable tie-line power flows between interconnected areas. By incorporating a frequency bias factor into the control strategy, AGC adjusts generator outputs to counteract frequency deviations and maintain scheduled power exchanges.

The frequency bias factor represents the sensitivity of the control area to frequency changes. Proper selection of this factor is essential for achieving effective coordination between control areas and minimizing ACE values.

Therefore, the ACE for area 1 is equal to Equation (18) [26]:

$$ACE_1 = \Delta P_{12} + B_1 \Delta f \tag{18}$$

With B1 given in Equation (19):

$$B_1 = \beta_1 = \frac{1}{R_1} + D_1 \tag{19}$$

Similarly for region 2 Equations (20) and (21) hold [26]:

$$ACE_2 = \Delta P_{21} + B_2 \Delta f \tag{20}$$

$$B_2 = \beta_2 = \frac{1}{R_2} + D_2 \tag{21}$$

Block diagram of a two-zone system with complementary control is presented in Figure 28.

2.18. Basis for Selecting the Bias Coefficient

The selection of the frequency bias coefficient is based on factors such as the system's inertia, load characteristics, and the desired level of inter-area coordination. An appropriately chosen bias coefficient ensures stable operation and minimizes the impact of frequency deviations on tie-line power flows. The bias coefficient must be carefully calibrated for each control area, taking into account its unique operating conditions and interconnections with neighboring areas.

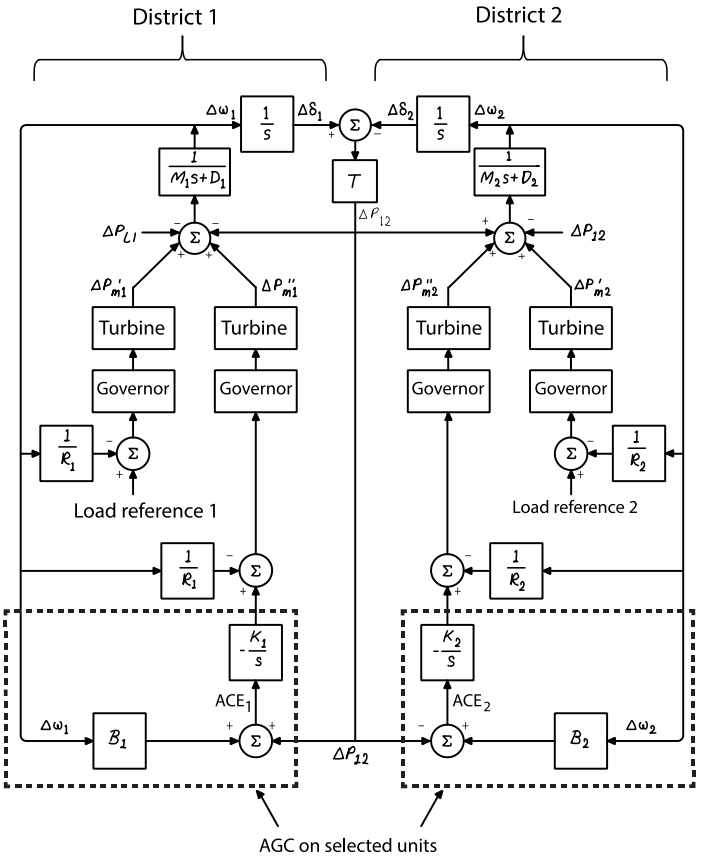


Figure 28. Block diagram of a two-zone system with complementary control [26].

2.19. Control of Multiple Generators in Each Area

In a multi-generator control area, AGC ensures that the output of each generator is adjusted proportionally to its capacity while maintaining the overall balance between generation and demand. The coordination among generators is achieved through proportional control mechanisms, such as droop settings, which distribute the load changes equitably among all generators.

This proportional load distribution minimizes the risk of overloading any single generator and ensures stable operation across the entire control area. Additionally, advanced AGC algorithms further enhance this process by dynamically optimizing the contribution of each generator based on real-time system conditions.

If we denote the participation coefficient for generator i by αi, then Equation (22) holds [13]:

$$\sum_i \alpha_i = 1 \tag{22}$$

In this case, the AGC block diagram for each region can be considered as Figure 29 [13].

2.20. AGC in Three-Area Power Systems

In three-area power systems, AGC extends its functionality to coordinate power flows and maintain frequency stability across three interconnected regions. Each area operates independently to some extent but relies on tie-line power exchanges to balance fluctuations in demand and generation. A general three-area network is depicted in Figure 30. The control strategy in three-area systems involves minimizing the ACE for each area while maintaining scheduled power flows along the tie-lines. This requires precise tuning of AGC parameters and effective communication between the control centers of the three areas.

2.21. General Operation of AGC

The general operation of AGC involves continuously monitoring the system's frequency and tie-line power flows, calculating the ACE for each control area, and adjusting generator outputs to minimize the ACE values. This process ensures that the system frequency is restored to its nominal value, and power exchanges between areas remain within scheduled limits.

AGC systems use various control techniques, including PI controllers, to achieve accurate and stable frequency regulation. In recent years, advanced control methods, such as fuzzy logic and neural networks, have also been integrated into AGC systems to enhance their performance under dynamic operating conditions. AGC for each region in general mode is given in Figure 31.

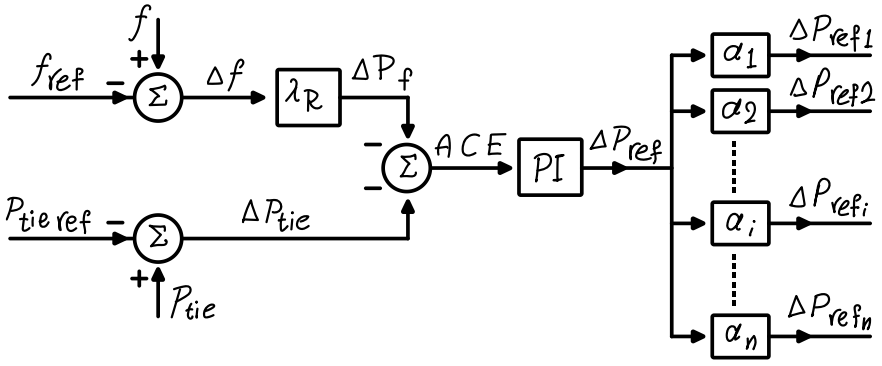


Figure 29. Block diagram of AGC in each zone for controlling multiple generators [13].

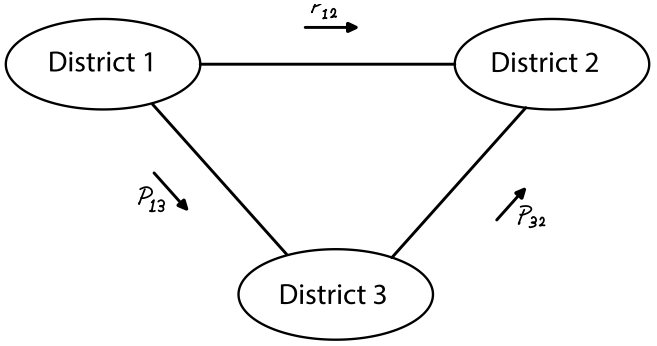


Figure 30. Three-area network [11].

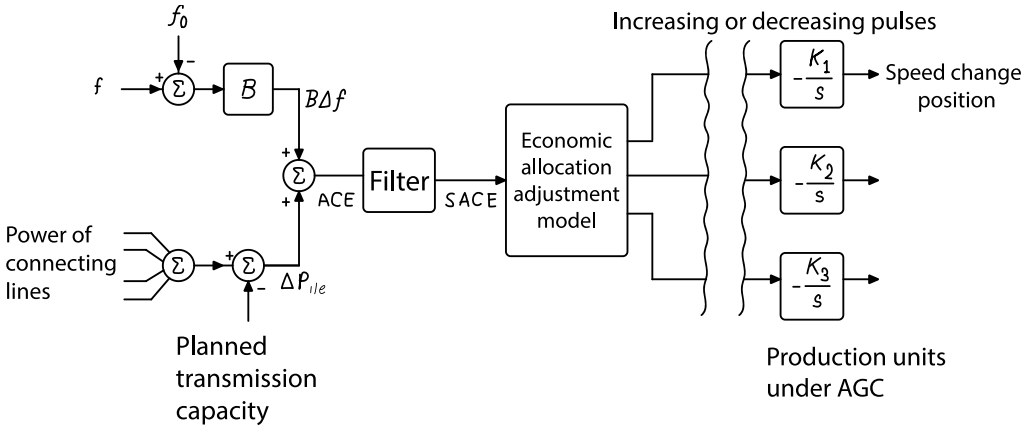


Figure 31. AGC for each region in general mode [11].

2.22. Filtering the ACE Signal

Filtering the ACE signal is an essential step in AGC systems to reduce the impact of high-frequency noise and transient disturbances on the control process. By applying suitable filters to the ACE signal, AGC systems can focus on long-term trends and avoid unnecessary adjustments caused by short-term fluctuations.

Proper filtering improves the stability and reliability of AGC systems, ensuring smooth and accurate frequency regulation across the power grid.

2.23. Intra-Area Automatic Control

Intra-area automatic control focuses on maintaining frequency stability and load sharing within a single control area. This involves coordinating the outputs of all generators in the area to ensure that the total generation matches the load demand.

The control process relies on real-time monitoring of frequency deviations and generator outputs, with adjustments made to restore the balance between generation and consumption. Advanced intra-area control systems also incorporate predictive algorithms to anticipate and respond to future load variations.

2.23.1. Performance Criteria for Control Systems

The performance of AGC systems is evaluated based on criteria such as response time, frequency deviation minimization, and the ability to maintain scheduled tie-line power flows. Key metrics include:

Settling time: The time required for the system to restore frequency and power flows to their nominal values after a disturbance.

Overshoot: The extent to which frequency or power flows exceed their nominal values during the restoration process.

Steady-state error: The remaining deviation in frequency or power flows after the system has stabilized.

By optimizing these performance criteria, AGC systems can achieve robust and reliable frequency regulation under a wide range of operating conditions.

3. Proposed Method in AGC System Based on Fuzzy PID Controller

This chapter introduces the proposed method for enhancing the performance of AGC systems using a fuzzy PID controller. Traditional AGC systems, while effective under steady-state conditions, often struggle to maintain optimal performance under dynamic and rapidly changing operating conditions.

By integrating fuzzy logic with conventional PID control, the proposed method aims to improve the adaptability and robustness of AGC systems. This hybrid approach combines the precise tuning capabilities of PID controllers with the intelligent decision-making features of fuzzy logic, enabling more effective frequency and power flow regulation.

3.1. AGC System Considering Excitation Systems

The excitation system plays a crucial role in maintaining the stability and performance of power systems. By controlling the voltage of the generator, the excitation system influences the reactive power output and, indirectly, the stability of the system frequency.

The proposed method incorporates the dynamic behavior of excitation systems into the AGC model. This integration allows for more accurate simulation of real-world operating conditions and enhances the effectiveness of the control strategy.

The key components of the proposed AGC system include:

A multi-stage fuzzy PID controller: Designed to handle dynamic operating conditions and optimize system response.

A filter (1 + PI): Added to improve stability and reduce noise in the control signals.

Real-time data monitoring: Ensures timely adjustments based on the system's current state.

3.2. Effectiveness of CES in Reducing Frequency Oscillations

3.2.1. Fast Response for Mitigating Frequency Deviation

The biggest challenge for AGC in modern grids is the speed of response to sharp and sudden load changes or fluctuations in renewable energy output. Thermal or hydraulic turbines are restricted by inertia and time limitations that prevent them from responding quickly to frequency oscillations (such as time delays in the governor and turbine).

Role of CES: CES systems can increase or decrease their power output in a fraction of a second. The moment a frequency deviation (Δf) occurs due to a generation deficit or surplus, CES immediately injects or absorbs the necessary power. This action occurs before the frequency deviation reaches critical values and before oscillations become large.

Advantage over Conventional AGC: In a system with conventional Fuzzy/PID control, one typically has to wait for the ACE to accumulate and the control signal to become sufficiently large. CES effectively eliminates this delay, drastically reducing the Settling Time and Overshoot.

3.2.2. Active Damping of Power Oscillations

When AGC relies solely on conventional generation units, the power adjustment necessary to correct the frequency can itself lead to power oscillations in the tie-lines.

Role of CES: By being placed in the control loop, CES acts as an Active Damper. The Fuzzy/PID controller can adjust its output signal so that CES absorbs small frequency and power oscillations, while the larger, slower thermal units remain responsible only for the more stable and longer-term adjustments (steady-state).

Therefore, by absorbing the initial shocks, the CES dynamically smooths the control system and improves inter-area power sharing stability.

3.2.3. Improved Performance in Nonlinear and Dynamic Environments

The integration of renewable energy sources inherently adds complexity and nonlinearity to the system. The proposed fuzzy controller (FPIDF (1 + PI)) is well-suited to this environment due to its high flexibility and adaptability.

Combination of fuzzy and CES: When the fuzzy controller, which possesses rule-based decision-making capability, sends its signal to a fast-response unit like CES, this creates an optimal combined performance. The fuzzy controller can quickly diagnose the situation based on input variables (such as frequency deviation and its rate of change) and issue the appropriate signal for power injection or absorption by CES. This combination ensures that the frequency quickly returns to its nominal value with less oscillation, even under dynamic operating scenarios and severe load changes (such as the states simulated at seconds 5 and 7).

In summary, by providing an immediate response, CES enables the AGC system to suppress frequency and power oscillations during the transient phase, paving the way for the stable and precise performance of more traditional controllers in the steady-state.

Simulation results demonstrate that the proposed method significantly outperforms traditional AGC systems in terms of frequency stability, settling time, and robustness against load disturbances. Figure 32 shows the schematic of the components of the proposed fuzzy PID controller.

3.2.4. Key Features of the Proposed Method

Enhanced Stability: The integration of fuzzy logic and PID control improves the system's ability to maintain frequency and power flow stability under dynamic conditions.

Adaptability: The fuzzy logic component enables the controller to adapt to changing system parameters and operating conditions.

Improved Performance Metrics: The proposed method reduces overshoot, minimizes steady-state error, and shortens settling time.

Applicability to Multi-Area Systems: The method can be extended to multi-area power systems, allowing for coordinated control of frequency and power flows across interconnected regions.

3.3. Simulation Setup and Results

To evaluate the performance of the proposed method, simulations were conducted using a multi-area power system model. The results were compared against conventional AGC systems under various operating scenarios, including:

Sudden load changes.

Inter-area power flow disturbances.

Dynamic variations in system parameters.

The proposed method consistently demonstrated superior performance, achieving faster frequency restoration and more stable power flow regulation compared to traditional AGC systems.

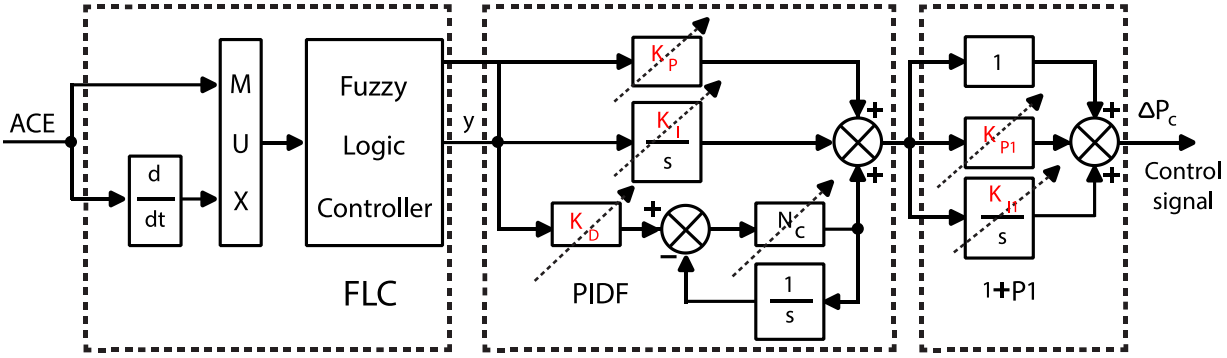


Figure 32. Schematic of the components of the proposed fuzzy PID controller.

3.4. Detailed Model of the Proposed AGC System

The proposed AGC system integrates a fuzzy PID controller with excitation system dynamics to achieve enhanced performance. Below are the primary components and their roles:

Fuzzy PID Controller:

The fuzzy PID controller combines the advantages of traditional PID control and fuzzy logic.

PID Control: Provides precise adjustment of generator outputs to maintain system frequency and power flow stability.

Fuzzy Logic: Enables the system to adapt to non-linear and dynamic operating conditions by applying a rule-based decision-making process.

The fuzzy PID controller includes:

Input variables: Frequency deviation and its rate of change.

Output variable: Control signal to adjust turbine input.

Fuzzy membership functions: Defined for input and output variables to enable smooth transitions between different operating states.

The Fuzzy Logic Controller (FLC) in the FPIDF system is responsible for adaptively tuning the PID parameters or generating an intelligent control signal. The core of this design comprises three stages: Fuzzification, Inference, and Defuzzification.

Fuzzification and Membership Functions

Fuzzification is the process where the precise, numerical values (crisp inputs) of the system's inputs are converted into Degrees of Membership within Fuzzy Sets. Based on previous explanations and Table 1, the FLC has two main inputs:

ACE: Which corresponds to the frequency deviation (Δf or Δω).

Rate of Change of ACE ($\frac{d}{dt}ACE$): Which indicates the speed of the system's movement toward stability or instability.

Figure 33 illustrates the Membership Functions defined for each of the inputs and outputs. These functions describe the degree to which an input value belongs to a particular fuzzy set. The most common functions used in Figure 35 are Triangular and Trapezoidal functions, which are popular due to their computational simplicity. To ensure full coverage of the input range, the domain of values for each input is divided into several fuzzy sets. There are typically seven sets in fuzzy PID controls, as shown in Table 1. The process of designing these functions involves determining the appropriate range of coverage (which is set based on the maximum permissible frequency deviation) and the appropriate overlap between the functions. The overlap is usually considered to be between 15% to 50% to provide a smooth transition between the rules.

Inference Rules

The Inference Rules (or the Fuzzy Rules in Table 1) form the core of the FLC's decision-making logic. These rules specify how the output signal is generated based on the fuzzified inputs and follow an IF-THEN format. The rules are structured as follows:

Rule i: IF ACE is Ai AND $\frac{d}{dt}ACE$ is Bi THEN Output is Ci

where Ai and Bi are the input Fuzzy Sets, and Ci is the output fuzzy set (e.g., ΔPc or parameter KP). Table 1 shows a 7×7 matrix containing 49 rules.

Rule-Setting Strategy (Based on AGC Principles)

The rules are designed based on power system control principles to drive the system toward zero error:

Rapid Correction Area (Matrix Corners):

If the error (ACE) is large and the rate of change ($\frac{d}{dt}ACE$) is exacerbating it, the system is highly unstable and requires a large and strong control command (LP or LN). For instance:

IF ACE is LP AND $\frac{d}{dt}ACE$ is LP THEN Output is LN

Overshoot Reduction Area (Diagonal Band):

If the error (ACE) is large but the rate of change ($\frac{d}{dt}ACE$) is working to reduce the error, the system is returning close to the nominal value. In this case, the control command must be weakened to prevent overshoot. For instance:

IF ACE is LP AND $\frac{d}{dt}ACE$ is MN THEN Output is Z or SP

Steady-State Area (Around the Center):

If both inputs (ACE and $\frac{d}{dt}ACE$) are close to zero, the control output should also be zero (Z) to prevent steady-state oscillation.

Defuzzification

After the rules are executed, multiple fuzzy outputs are generated. Defuzzification converts these fuzzy outputs into a single, precise control signal (ΔPc) that is then applied to the generator actuators.

For this purpose, the Center of Gravity (CoG) method or the Center of Sums method are the most widely used. In the CoG method, the output is calculated as the weighted average of the outputs of each rule to produce a smooth and continuous signal for application to the physical system.

4. The FPIDF Controller

The FPIDF controller combines the flexibility of fuzzy logic with the precision and speed of PID control, adding an auxiliary filter to ensure system stability. The FPIDF structure (Figure 32) is divided into three main components that work together in a cascaded manner:

4.1. FLC

This section is the intelligent core of the controller, responsible for adaptively tuning the PID parameters or generating an adaptive control signal based on non-linear decision-making rules. The primary inputs to the FLC are the ACE and its rate of change ($\frac{d}{dt}ACE$) (which, in the proposed model, correspond to the frequency deviation Δω and its rate of change). Membership functions (such as triangular or Gaussian in Figure 35) are defined for each input and output. These functions convert the numerical input values into fuzzy linguistic terms (such as "Large Negative," "Zero," or "Small Positive"). Next, based on the rule table (e.g., Table 1), the FLC produces an output (e.g., ΔKP, ΔKI, or a control factor). These rules are written in the "IF-THEN" format. For instance: If ACE is Large Positive (LP) and $\frac{d}{dt}ACE$ is Large Positive (LP), then the control output ΔPc will be Large Negative (LN) (to quickly reduce power). Finally, the linguistic output of the FLC is converted to a crisp value through Defuzzification, which is then used in the next section of the controller.

4.2. PID-F Section

This section preserves the classic structure of PID control, but its reference signal or gain parameters (KP, KI, KD) are dynamically adjusted by the FLC. Under normal and linear conditions, the PID controller provides the necessary accuracy and stability. During dynamic and nonlinear conditions, the FLC intervenes to adapt the PID parameters to reduce overshoot and accelerate the settling time. The output of this section is the signal generated to correct the frequency deviation.

Excitation System Integration:

The excitation system impacts reactive power control and indirectly stabilizes system frequency. The proposed method incorporates the dynamic characteristics of the excitation system to improve the accuracy of the control strategy.

Filter (1 + PI):

A filter is included to suppress noise and reduce high-frequency oscillations in the control signals. This ensures smoother operation and enhances the stability of the AGC system.

This filter is combined with a PI block, which includes a proportional gain (P) and an integral element (I) with their own specific gains. Its purpose is to filter out transient noise and provide a smoother control response without seriously compromising the speed of response. The addition of this filter is especially crucial when the controller commands fast-response resources (such as CES); it ensures that the control commands being sent are not oscillatory or unstable.

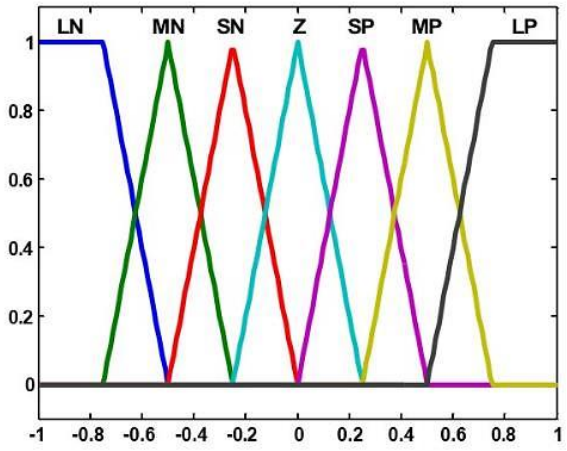


Figure 33. Membership functions of the proposed fuzzy system [27].

Table 1. Table of fuzzy rules between inputs and outputs [27].

ACE	ACE derivative						
	LN	MN	SN	Z	SP	MP	LP
LN	LP	LP	LP	MP	MP	SP	Z
MN	LP	MP	MP	MP	SP	Z	SN
SN	LP	MP	SP	SP	Z	SN	MN
Z	MP	MP	SP	Z	SN	MN	MN
SP	MP	SP	Z	SN	SN	MN	LN
MP	SP	Z	SN	MN	MN	MN	LN
LP	Z	SN	MN	MN	LN	LN	LN

4.3. Filter Transfer Function

The transfer function of a simple PI controller in the Laplace domain (s) is given as [6]:

$$G_{PI}(s) = K_P + \frac{K_I}{s} \tag{23}$$

In the (1 + PI) filter, the transfer function is as follows (assuming a gain of 1 in the direct path):

$$G_{Filter}(s) = 1 + \left(K_P + \frac{K_I}{s} \right) = \left(1 + K_P \right) + \frac{K_I}{s} \tag{24}$$

If we define $K_F = 1 + K_P$ and $T_I = \frac{K_F}{K_I}$ (the integral time constant), it can be written in the standard form of a Lead-Lag filter:

$$G_{Filter}(s) = K_F \left(1 + \frac{1}{T_I s} \right) = K_F \frac{T_I s + 1}{T_I s} \tag{25}$$

This filter creates a zero at $s = \frac{-1}{T_I}$ and a pole at the origin (s = 0).

4.4. Performance in Noise Reduction and Stability Improvement

Reduction of High-Frequency Oscillations (Filtering):

The (1 + PI) filter acts like a Lag Compensator or a Low-Pass Filter at high frequencies, which can help reduce high-frequency noise and oscillations.

The integral effect (1/s) has a very small contribution to the Signal Magnitude (when $|s| \to \infty$) at high frequencies. Consequently, high-frequency signals mainly pass through the gain KF. Although this filter is not a strong low-pass filter on its own (due to the lack of a second pole), its damping effects are enhanced when combined with the main controller (FPID). Its primary goal is not high-frequency noise filtering, but rather phase and gain correction at intermediate frequencies.

Stability Improvement (Phase and Gain Correction):

The main function of this filter is to adjust the system's open-loop characteristics near the crossover frequency to enhance stability. System stability is measured by the Phase Margin (PM) and Gain Margin (GM). The objective is to increase these margins.

Effect of the Pole and Zero:

Pole at the origin (s = 0): This pole reduces the PM at lower frequencies but drives the steady-state error to zero (which was already guaranteed by the main controller).

Zero at $s = \frac{-1}{T_I}$: This zero becomes active at higher frequencies and introduces a Phase Boost to the system.

$$\Phi_{max} = arctan(\omega T_I) \tag{26}$$

This phase increase leads to an increase in the PM at the crossover frequency. An increased Phase Margin signifies greater stability and a reduction in overshoot in the step response.

Steady-State Gain

$$\lim_{s \to 0} G_{Filter}(s) \to \infty \tag{27}$$

In terms of the steady-state, this filter has an infinite gain due to the presence of the integrator (pole at the origin), which helps in achieving zero Steady-State Error.

Our model is a two-zone renewable hybrid power plant with three fuzzy controllers, PID and PI, and is simulated in Simulink of MATLAB 2018B. In Ref. [27], only frequency stabilization is investigated, but we also consider the sharp load changes at 5 seconds for the first zone and 7 seconds for the second zone. The load change value is equal to 0.1875 pu. This disturbance is applied suddenly to the system at seconds 5 and 7, and the performance of the proposed controller in stabilizing the system during this disturbance is tested.

5. Simulation Results and Discussion

As can be seen in the figures, we examined the model in three cases:

- The load change occurs only in zone 1 and at second 5.
- The load change occurs only in zone 2 and at second 7.
- The load change occurs in both zone 1 and zone 2 and at second 5 and 7 respectively.

(The red graph is for zone 1 and the blue graph is for zone 2) As can be seen, the difference in the frequency of the three cases is well resolved. Structure of the simulated model is shown in Figure 34. Also, Figure 35 provides the results obtained from simulation. Figure 36 presents the block diagram representation of the proposed design in the simulated structure.

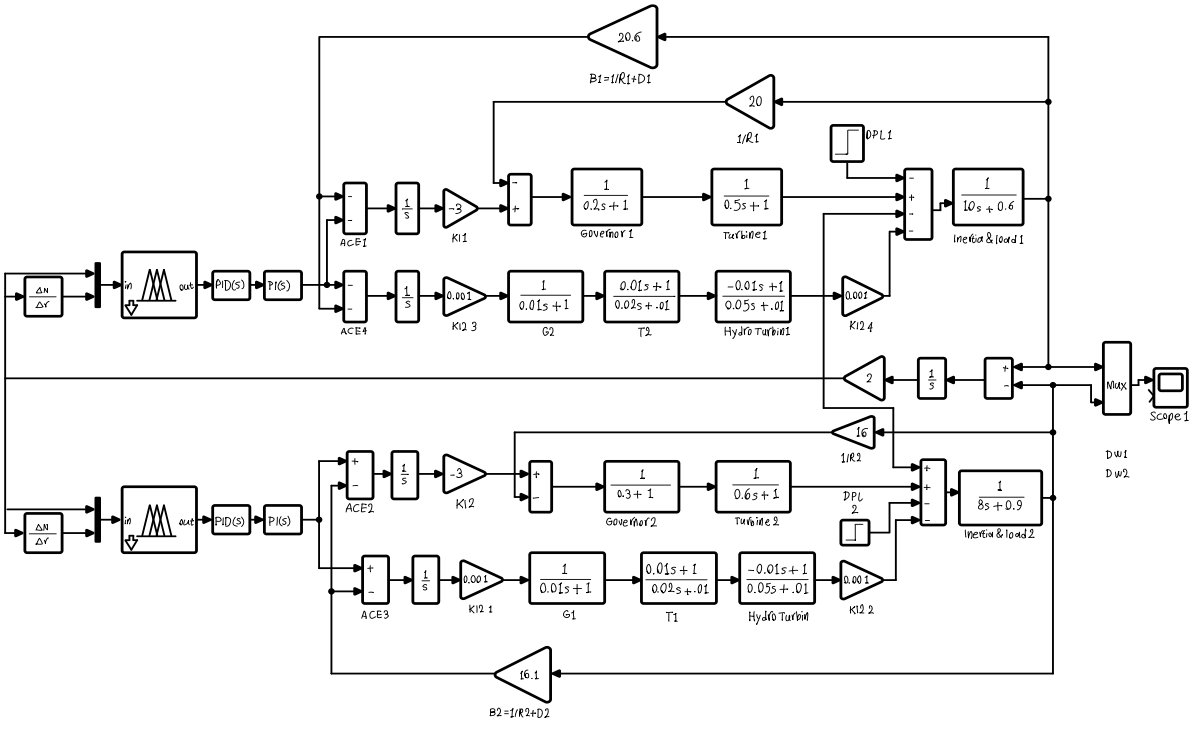
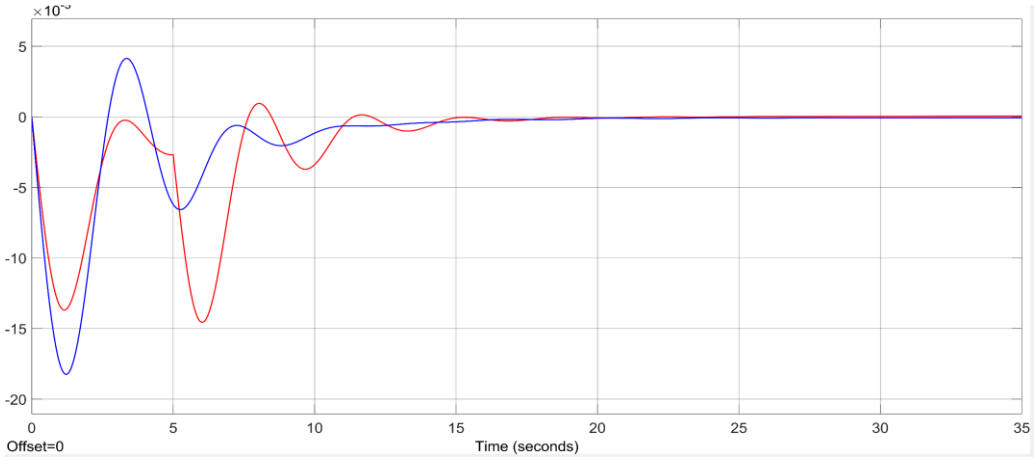
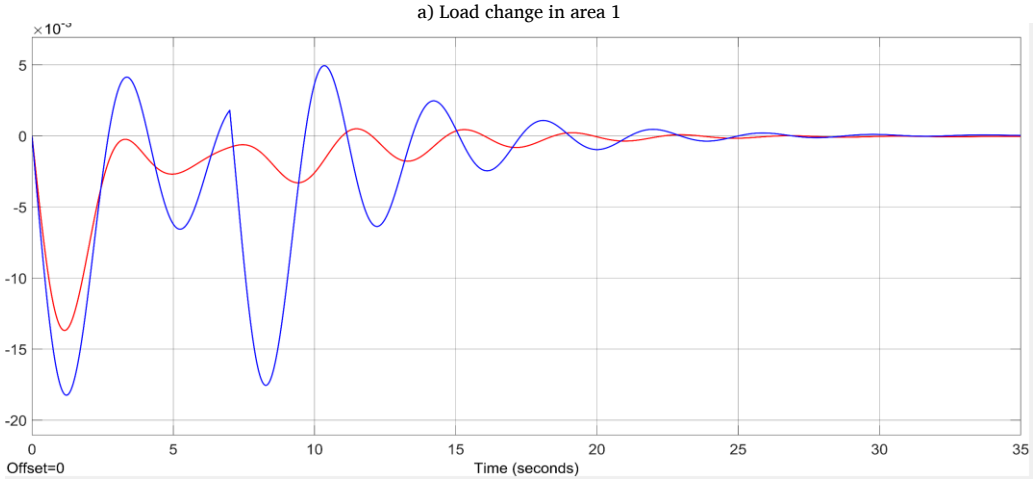


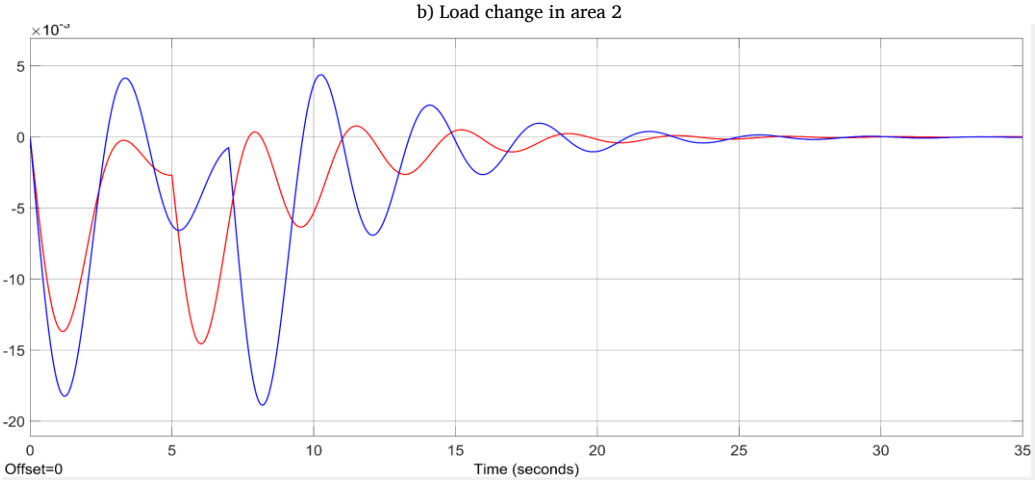
Figure 34. Structure of the simulated model.



a) Load change in area 1



b) Load change in area 2



c) Load change in zones 1 and 2

Figure 35. Results obtained from simulation**.**

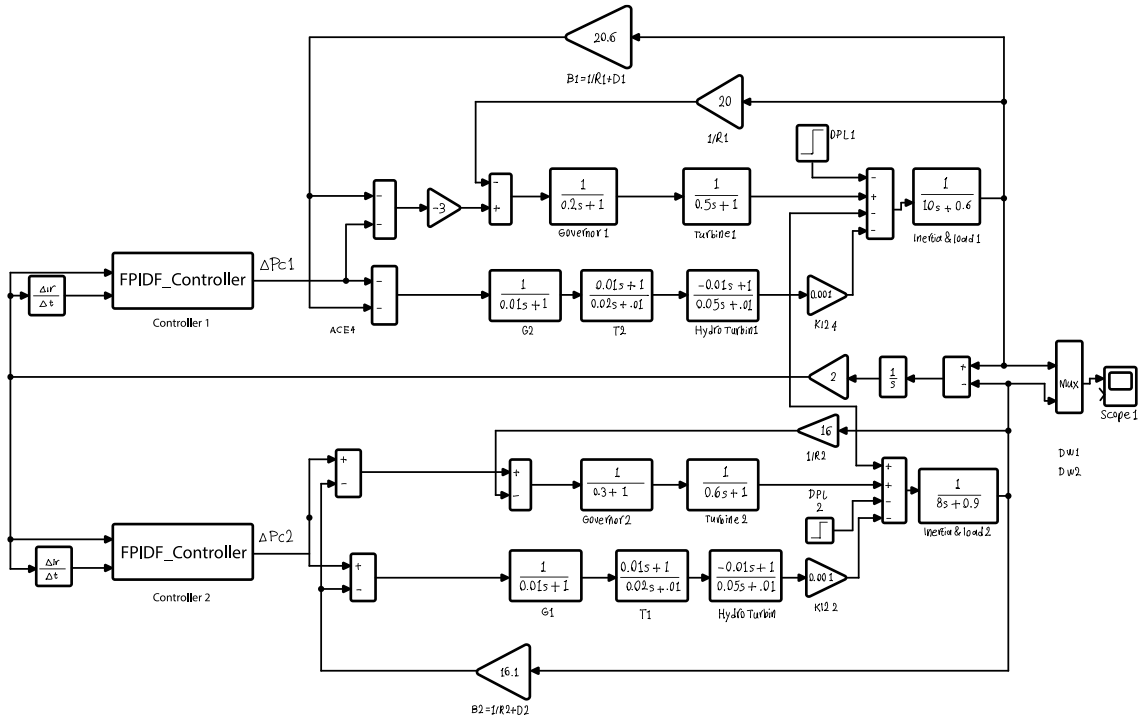


Figure 36. Block diagram representation of the proposed design in the simulated structure.

According to the simulation results, the values for Overshoot, Settling Time, and Steady-State Error under various scenarios are summarized in Table 2.

The negative sign for Δf indicates a decrease in frequency due to an increase in load. A positive sign for ΔPtie means power flows out of the area, while a negative sign means power flows into the area.

Even in the severe scenario, where there are two consecutive disturbances, the overshoot values remain within approximately 2% of the nominal frequency (e.g., 50 or 60 Hz), which indicates a very good performance of the controller.

If the nominal frequency is 50 Hz, 0.015 p.u. Hz is an approximate deviation of 0.75 Hz.

5.1. Comparison with Other Control Approaches

The proposed method, in the worst-case scenario where load changes occur sequentially in areas 1 and 2, has a settling time of 8 seconds. Ref. [27], which uses a controller similar to the proposed method, has a settling time of 12.33 seconds for the frequency of area 1 (Δf1). Similarly, the settling time for other controllers examined in [27], such as ICA: FPIDF, is 14.27 seconds. This signifies a 35% improvement in the stabilization speed of the power system after a disturbance when using the proposed control scheme.

Table 3 presents the Overshoot values for each article along with its reference number. In this paper, the maximum overshoot occurred in Δf2 in Figure 35(c). This overshoot is lower than the values reported in the articles listed in the table, and its percentage improvement is also included in the table.

6. Conclusion

The integration of renewable energy sources into modern power systems introduces inherent complexity and nonlinearity, particularly under high-load and dynamic operating conditions. These systems frequently experience significant frequency deviations and power oscillations, especially during periods of generation shortfall. Moreover, continuous fluctuations in load demand exacerbate variations in grid frequency, power flow across transmission lines, and the output of generation units.

To mitigate these challenges, AGC mechanisms are employed within power grids to maintain system frequency at its nominal value and to regulate scheduled inter-area power exchanges. The core of AGC operation lies in the ACE, a control variable designed to correct deviations in frequency and tie-line power flows. Achieving a real-time balance between generation and demand in such a dynamic environment is highly complex. Therefore, the adoption of advanced control strategies and fast-responding ESS becomes imperative. Among various ESS technologies, CESs have demonstrated significant potential in maintaining frequency stability and mitigating power oscillations caused by abrupt load variations.

Table 2. FPIDF Controller Performance Analysis.

Scenario	Signal Under Review	Overshoot (p.u. × 10 − 3 Hz)	Settling Time	Steady-State Error
Figure 35 (a): Step Load Change in Area 1 (at t = 5s)	Δf1	−17 (Max negative peak)	Fast (5 seconds after disturbance)	Zero (Effective integral action)
	Δf2	−8 (Max negative peak)	Fast (4 seconds after disturbance)	Zero
	ΔPtie	+4 (Max positive peak)	Fast (5 seconds after disturbance)	Zero
Figure 35 (b): Step Load Change in Area 2 (at t = 7s)	Δf1	−8 (Max negative peak)	Fast (4 seconds after disturbance)	Zero
	Δf2	−18 (Max negative peak)	Fast (5 seconds after disturbance)	Zero
	ΔPtie	−4 (Max negative peak)	Fast (5 seconds after disturbance)	Zero
Figure 35 (c): Sequential Load Changes in Area 1 (t = 5s) & Area 2 (t = 7s)	Δf1	−18 (Largest negative peak)	Longer (8 seconds after 2nd disturbance)	Zero (Despite high stress)
	Δf2	−19 (Largest negative peak)	Longer (8 seconds after 2nd disturbance)	Zero
	ΔPtie	+5 (Largest positive peak)	Longer (8 seconds after 2nd disturbance)	Zero

Table 3. Percentage improvement in overshoot for the proposed method.

The Overshoot in Δf2 in Figure 37(c) = -19×10^{-3}

Ref.	Overshoot ($\times 10^{-3}$ Hz)	Stability Improvement (%)
[10]	20	5
[11]	$\pm$ 20	5
[15]	-43.66	56
[16]	413	95
[2]	-254	93
[22]	-106	82
[4]	-106	82
[5]	-48	60

This study explores the impact of CES units on the performance of AGC in a robust, interconnected power network. Recognizing the superior adaptability of fuzzy logic techniques in uncertain and nonlinear environments, a novel multi-stage fuzzy Proportional-Integral-Derivative controller integrated with a filter, designated as FPIDF (1 + PI), is proposed. This intelligent control scheme is developed to enhance the stability, responsiveness, and overall effectiveness of AGC functions. Simulation results confirm the superior performance of the proposed FPIDF (1 + PI) controller compared to conventional control strategies, demonstrating its efficacy in managing frequency deviations and maintaining system stability in renewable-integrated power systems.

7. Applications and future horizons

The proposed method has the potential to be implemented in other power systems connected to renewable sources such as photovoltaic units as well as thermal power plants. This method can be widely used in modern power grids and industrial systems that require precise power control and stability. It is suggested that further research be conducted in the future to optimize the controller parameters in larger and more complex networks. Also, examining the system performance in the presence of greater uncertainties, such as severe load changes or the addition of new energy sources, can help to further improve this method.

Attachments

A. Area Key Parameters

These parameters define the general dynamic response of each control area (Area i) [8].

Parameter	Symbol	Typical Value (p.u./Hz)	Basis of Selection and IEEE Compatibility
Equivalent Power Plant Gain	KP	120	Derived from the standard IEEE model for AGC. This value is the inverse of the damping coefficient (D) divided by the nominal frequency ($\approx 2 \times D \times Heq$).
Equivalent Power Plant Time Constant	TP	20 seconds	Represents the net mechanical-electrical time delay of the power plant and load response to frequency changes. This is a standard academic reference value for LFC studies in thermal systems.
Frequency Bias Factor	B	$\beta = \frac{1}{R} + D$	IEEE Standard Value: The area frequency bias is calculated as B = R1 + D. A common value is B = 0.425 (assuming R = 0.05 and D = 0.0083) and is mandatory to ensure proper steady-state stability and power exchange between areas.
Controller Integral Gain	KI	Variable (0.01 to 0.5)	This is a tuned parameter for controller (PI or FPIDF). It is determined through optimization methods (like PSO or ITAE) and has no fixed standard value.

B. Governor/Thermal Turbine Parameters

These parameters follow the standard modeling of governors and thermal turbines [8].

Parameter	Symbol	Typical Value (seconds)	Basis of Selection and IEEE Compatibility
Governor Time Constant	TG	0.08	Derived from standard governor models (e.g., IEEE's Reheat Governor Model).
Turbine Time Constant	TT	0.3 to 0.5	Represents the thermal and mechanical lag of the turbine in response to valve changes. This value is consistent with the standard steam turbine model used in power system dynamics studies.
Speed Droop Setting	R	0.05	This is a standard and mandatory value representing a 5% speed droop. It is crucial for ensuring correct load distribution among generators in an area during Primary Frequency Control.

C. Inter-Area Tie-Line Parameters

These parameters define the interaction and power exchange between Area 1 and Area 2 [8].

Parameter	Symbol	Typical Value	Basis of Selection
Tie-Line Synchronizing Coefficient	T12	$\frac{2\pi P_{rated}}{X_{tie}}$	Often represented as $T_{12} = \frac{2\pi}{X_{tie}}$ (in units of p.u. power / radian), this parameter indicates the power required to create a 1-radian change in the phase angle between the two areas. A common academic value for a simplified two-area system is 0.545 p.u.

References

[1] N. Li, C. Zhao, and L. Chen, "Connecting Automatic Generation Control and Economic Dispatch from an Optimization View," *IEEE Transactions on Control of Network Systems*, vol. 3, no. 3, pp. 254–264, 2016.

[2] U. K. Rout, R. K. Sahu, and S. Panda, "Design and Analysis of Differential Evolution Algorithm Based Automatic Generation Control for Interconnected Power System," *Ain Shams Engineering Journal*, vol. 4, no. 3, pp. 409–421, 2013.

[3] R. Schulte, "An Automatic Generation Control Modification for Present Demands on Interconnected Power Systems," *IEEE Transactions on Power Systems*, vol. 11, no. 3, pp. 1286–1294, 1996.

[4] R. K. Sahu, S. Panda, and S. Padhan, "A Hybrid Firefly Algorithm and Pattern Search Technique for Automatic Generation Control of Multi Area Power Systems," *International Journal of Electrical Power & Energy Systems*, vol. 64, pp. 9–23, 2015.

[5] S. Sridhar and M. Govindarasu, "Model-Based Attack Detection and Mitigation for Automatic Generation Control," *IEEE Transactions on Smart Grid*, vol. 5, no. 2, pp. 580–591, 2014.

[6] N. Cohn, "Some Aspects of Tie-Line Bias Control on Interconnected Power Systems," *Transactions of the American Institute of Electrical Engineers. Part III: Power Apparatus and Systems*, vol. 75, no. 3, 1956.

[7] L. K. Kirchmayer, *Economic Control of Interconnected Systems*, John Wiley & Sons, 1959.

[8] B. O'hara and A. Petrick, *IEEE 802.11 Handbook: A Designer's Companion*, IEEE Standards Association, 2005.

[9] J. E. Van Ness, "Root Loci of Load Frequency Control Systems," *IEEE Transactions on Power Apparatus and Systems*, vol. 82, no. 5, pp. 712–726, 1963.

[10] O. Elgerd, and C. Fosha, "Optimum Megawatt-Frequency Control of Multiarea Electric Energy Systems," *IEEE Transactions on Power Apparatus and Systems*, vol. PAS-89, no. 4, pp. 556–563, 1970.

[11] C. Fosha, and O. Elgerd, "The Megawatt-Frequency Control Problem: A New Approach Via Optimal Control Theory," *IEEE Transactions on Power Apparatus and Systems*, vol. PAS-89, no. 4, pp. 563–577, 1970.

[12] S. P. Singh, T. Prakash, V. Singh, and M. G. Babu, "Analytic Hierarchy Process Based Automatic Generation Control of Multi-Area Interconnected Power System Using Jaya Algorithm," *Engineering Applications of Artificial Intelligence*, vol. 60, pp. 35–44, 2017.

[13] M. Toulabi, S. Bahrami, and A. M. Ranjbar, "Application of Edge Theorem for Robust Stability Analysis of a Power System with Participating Wind Power Plants in Automatic Generation Control Task," *IET Renewable Power Generation*, vol. 11, no. 7, pp. 1049–1057, 2017.

[14] G. Sharma, I. Nasiruddin, K. R. Niazi, and R. C. Bansal, "Automatic Generation Control (AGC) of Wind Power System: A Least Squares-Support Vector Machine (LS-SVM) Radial Basis Function (RBF) Kernel Approach," *Electric Power Components and Systems*, vol. 46, no. 14-15, pp. 1621–1633, 2018.

[15] A. Behera, T. K. Panigrahi, A. K. Sahoo, and P. K. Ray, "Hybrid ITLBO-DE Optimized Fuzzy PI Controller for Multi-Area Automatic Generation Control with Generation Rate Constraint," *Smart Innovation, Systems and Technologies*, pp. 713–722, 2017.

[16] M. A. Elhosseini, R. A. El Sehiemy, A. H. Salah, and M. A. Abido, "Modeling and Control of an Interconnected Combined Cycle Gas Turbine Using Fuzzy and ANFIS Controllers," *Electrical Engineering*, vol. 100, no. 2, pp. 763–785, 2017.

[17] J. R. Nayak, B. Shaw, and B. K. Sahu, "Application of Adaptive-SOS (ASOS) Algorithm Based Interval Type-2 Fuzzy-PID Controller with Derivative Filter for Automatic Generation Control of an Interconnected Power System," *Engineering Science and Technology, an International Journal*, vol. 21, no. 3, pp. 465–485, 2018.
[18] S. A. Priyadarsini, P. M. Mary, and W. Iruthayarajan, "Automatic Generation Control in Deregulated Power System Using Genetic Algorithm Optimized Fuzzy Controller," *Applied Mathematics & Information Sciences*, vol. 11, no. 2, pp. 479–487, 2017.
[19] Y. Sharma, and L. C. Saikia, "Automatic Generation Control of a Multi-Area ST – Thermal Power System Using Grey Wolf Optimizer Algorithm Based Classical Controllers," *International Journal of Electrical Power & Energy Systems*, vol. 73, pp. 853–862, 2015.
[20] A. Sahu, and S. K. Hota, "Performance Comparison of 2-DOF PID Controller Based on Moth-Flame Optimization Technique for Load Frequency Control of Diverse Energy Source Interconnected Power System," *2018 Technologies for Smart-City Energy Security and Power (ICSESP)*, pp. 1–6, 2018.
[21] A. Panda, "Automatic Generation Control of Two Area Power System Using Modified Bacteria Foraging Algorithm," *International Journal of Emerging Technology and Engineering Research*, vol. 6, no. 3, pp. 27–30, 2018.
[22] D. Guha, P. K. Roy, and S. Banerjee, "Study of Differential Search Algorithm Based Automatic Generation Control of an Interconnected Thermal-Thermal System with Governor Dead-Band," *Applied Soft Computing*, vol. 52, pp. 160–175, 2017.
[23] P. Dash, L. C. Saikia, and N. Sinha, "Automatic Generation Control of Multi Area Thermal System Using Bat Algorithm Optimized PD–PID Cascade Controller," *International Journal of Electrical Power & Energy Systems*, vol. 68, pp. 364–372, 2015.
[24] K. Jagatheesan, B. Anand, et al., "Design of a Proportional-Integral-Derivative Controller for an Automatic Generation Control of Multi-Area Power Thermal Systems Using Firefly Algorithm," *IEEE/CAA Journal of Automatica Sinica*, vol. 6, no. 2, pp. 503–515, 2019.
[25] M. K. Debnath, J. R. Padhi, P. Satapathy, and R. K. Mallick, "Design of Fuzzy-PID Controller with Derivative Filter and Its Application Using Firefly Algorithm to Automatic Generation Control," *2017 6th International Conference on Computer Applications in Electrical Engineering-Recent Advances (CERA)*, pp. 353–358, 2017.
[26] S. R. Khuntia, and S. Panda, "Simulation Study for Automatic Generation Control of a Multi-Area Power System by ANFIS Approach," *Applied Soft Computing*, vol. 12, no. 1, pp. 333–341, 2012.
[27] Y. Arya, "AGC of PV-Thermal and Hydro-Thermal Power Systems Using CES and a New Multi-Stage FPIDF-(1 + PI) Controller," *Renewable Energy*, vol. 134, pp. 796–806, 2019.
[28] F. Amiri, and S. Sadr, "Designing a New Control Method to Improve the LFC Performance of the Multi-Area Power System Considering the Effect of Offshore Wind Farms on Frequency Control," *International Journal of Energy Research*, vol. 2025, no. 1, 2025.
[29] F. Amiri, M. Eskandari, and M. H. Moradi, "Improved Load Frequency Control in Power Systems Hosting Wind Turbines by an Augmented Fractional Order PID Controller Optimized by the Powerful Owl Search Algorithm," *Algorithms*, vol. 16, no. 12, 539, 2023.
[30] F. Amiri and M. H. Moradi, "Improvement of Frequency Stability in the Power System Considering Wind Turbine and Time Delay," *Journal of Renewable Energy and Environment*, vol. 10, no. 1, pp. 9–18, 2023.

Declaration of competing interest

The authors declare that they have no known competing financial interests or personal relationships that could have appeared to influence the work reported in this paper. The ethical issues, including plagiarism, informed consent, misconduct, data fabrication and/or falsification, double publication and/or submission, redundancy, have been completely observed by the authors.

Bibliography



Asaad Shemshadi was born on Nov 1, 1979. He received the B.Sc. degree from the Shiraz University, in 2003, the M.Sc. degree from the Kashan University, Iran in 2007, and PhD degree from Khaje Nasir Toosi University of Technology in 2014, all in Electrical engineering. His research interests are: Vacuum Interrupters design and analysis, high voltage simulations, thermal plasma modeling, high voltage equipment design, transients in vacuum arc quenching, renewable energies and pulsed power.
Email: shemshadi@arakut.ac.ir
ORCID: 0000-0002-7271-9933
Contribution Statement: Conceptualization, Data curation, Formal analysis, Investigation, Methodology, Resources, Software, Supervision, Validation, Visualization, Writing - original draft, Writing-review & editing.



Mehdi Payamani was born in Iran in 1998. He received his M.Sc. degree in Electrical Engineering with a specialization in Power Systems from Arak University of Technology, Arak, Iran, in 2025. His research interests include load frequency control, power system protection, and smart grid technologies. His academic work is primarily focused on control and stability enhancement in modern power systems.
Email: mhd.payamani@gmail.com
ORCID: 0009-0006-3457-9286
Contribution Statement: Conceptualization, Data curation, Formal analysis, Investigation, Methodology, Resources, Software, Validation, Visualization, Writing - original draft, Writing-review & editing.